

For Reference


NOT TO BE TAKEN FROM THIS ROOM

For Reference

NOT TO BE TAKEN FROM THIS ROOM

Ex LIBRIS
UNIVERSITATIS
ALBERTAENSIS





Digitized by the Internet Archive
in 2018 with funding from
University of Alberta Libraries

<https://archive.org/details/Chudobiak1962>

THE UNIVERSITY OF ALBERTA

AN EXPERIMENTAL STUDY OF AXI-SYMMETRIC INVERTED
EXTRUSION AND PIERCING

A THESIS

SUBMITTED TO THE FACULTY OF GRADUATE STUDIES
IN PARTIAL FULFILMENT OF THE REQUIREMENTS FOR THE DEGREE OF
MASTER OF SCIENCE

DEPARTMENT OF MECHANICAL ENGINEERING

by

JOSEPH M. CHUDOBIAK, B.Sc. (Alberta)

EDMONTON, ALBERTA

APRIL, 1962

ABSTRACT

The purpose of the experimental work of this thesis is to compare the die pressures of axi-symmetric inverted extrusion and piercing both with each other and with ideal die pressures. Also, the common assumption that the mean equivalent strain imparted to a material in a given working operation does not depend on its work-hardening characteristics or its saturation stress is investigated.

The metal used for these experiments was 0.06 percent tellurium lead in both the fully-hardened and annealed states.

Despite the fact that piercing involves the formation of a doubly connected cross-section, it was found, that for a given reduction the die pressures of axi-symmetric piercing were lower than those for axi-symmetric extrusion.

Deformation efficiencies for the extrusion and piercing of cold-worked tellurium lead were found to vary almost linearly with reduction.

Evidence was obtained which indicated that the assumption regarding mean equivalent strain is not too accurate.

Measurement of the frictional drag occurring between the container wall and the moving part of a billet being pierced showed that this drag is not necessarily small, even with proper lubrication.

ACKNOWLEDGMENTS

The author wishes to extend his appreciation to Dr. J.B.Haddow for supervising this thesis.

He would also like to thank Dr. G.Ford and Wing Commander B.Riedel for their assistance in making his graduate studies possible.

TABLE OF CONTENTS

CHAPTER	PAGE
1. INTRODUCTION.....	1
Description of the Processes.....	1
Theoretical Considerations.....	2
2. FORMULAS FOR THE PLANE STRAIN AND AXI-SYMMETRIC PROCESSES.	3
Experimental Comparison of Plane Strain and	
Axi-Symmetry.....	3
Empirical Relations for Axi-Symmetry.....	3
3. USE OF AVERAGE YIELD STRESS FOR WORK-HARDENING MATERIALS..	6
Explanation of Method of Average Yield Stress.....	6
Computation of Average Stress from the Stress-	
Strain Diagram.....	8
Experimental Justification for the Use of an	
Averaged Stress.....	9
4. DETERMINATION OF BOUNDS FOR THE FORMING LOADS.....	11
Concept of Bounds on P.....	11
Application of Bounding Techniques to Piercing.....	11
Neglect of Friction in Piercing.....	12
5. APPARATUS AND MATERIAL.....	13
Inverted Extrusion Apparatus.....	13
Piercing Apparatus.....	13
Billet Forming Apparatus.....	14
Billet Preparation.....	13
6. STRESS-STRAIN COMPRESSION TEST.....	20
Discussion of the Compression Test.....	20
Compression Test Procedure.....	21

CHAPTER	PAGE
7. EXPERIMENTAL PROCEDURE.....	24
Experimental Procedure--Piercing.....	24
Experimental Procedure--Extrusion.....	25
8. EXPERIMENTAL RESULTS AND DISCUSSION.....	26
Autographic Diagrams.....	26
Friction Results.....	35
Stress-Strain Diagrams.....	36
Pressure-Reduction Diagrams.....	38
Mean Equivalent Strains.....	42
Ideal Deformation Efficiency.....	45
9. CONCLUSIONS.....	48
BIBLIOGRAPHY.....	51

LIST OF FIGURES

FIGURE	PAGE
1. Inverted Extrusion Apparatus.....	15
2. Piercing Apparatus.....	16
3. Billet Forming Apparatus.....	17
4. Compression Sub-Press.....	22
5. Autographic Diagrams for Inverted Extrusion of Annealed Tellurium Lead.....	27
6. Autographic Diagrams for Piercing of Annealed Tellurium Lead.....	28
7. Autographic Diagrams for Inverted Extrusion of Fully-Hardened Tellurium Lead.....	29
8. Autographic Diagrams for Piercing of Fully-Hardened Tellurium Lead.....	30
9. Initiation of Unsteady State.....	32
10. Cavity Formation--Extrusion.....	33
11. Cavity Formation--Piercing.....	33
12. Photograph of Grid Movement in Check for Dead Metal--Extrusion.....	34
13. Piercing Apparatus in Place on Baldwin Testing Machine.....	34
14. Stress-Strain Diagrams for Tellurium Lead.....	37
15. Pressure-Reduction Diagrams for Fully-Hardened Tellurium Lead.....	39
16. Pressure-Reduction Diagrams for Annealed Tellurium Lead.....	40

FIGURE

PAGE

17. Mean Equivalent Strains for Fully-Hardened Tellurium

Lead..... 43

18. Comparison of Experimental and Mean Equivalent

Plastic Work-Annealed Tellurium Lead..... 44

19. Deformation Efficiencies for Fully-Hardened

Tellurium Lead..... 47

CHAPTER 1

INTRODUCTION

The two metal forming processes considered in this experimental investigation were axi-symmetric inverted extrusion and piercing.

1.1 Description of the Processes

Figure 1 shows the essentials of an axi-symmetric inverted extrusion process. A cylindrical billet is constrained in the container, and as the die is advanced the metal is forced to flow plastically through the die orifice, producing a cylindrical bar of reduced cross-sectional area. Note that there is no relative motion between the billet and the container wall, except in the immediate vicinity of the die.

Axi-symmetric inverted extrusion is to be contrasted with direct extrusion in which the die is held stationary in the container and the billet is advanced towards the die. The load required to advance the billet in direct extrusion is greater than that required to advance the die in inverted extrusion by the magnitude of the frictional resistance between the container wall and billet.

A simple axi-symmetric piercing apparatus is shown in Fig. 2. A cylindrical billet is constrained in the container and is converted into an annular cross-section as the punch is advanced.

For both forming processes described it is obvious that the deformation of the particles in any meridian plane may be considered as typical of the whole, hence the term axi-symmetric.

Using die area to refer to either the extrusion die face area or the piercing punch area then the reduction of area r is defined as

$$r = \frac{\text{die area}}{\text{billet area}} = \frac{a}{A} .$$

If the billet is of sufficient length it is to be expected that the die load, L , required to advance the die at a given rate, should attain a steady value. This steady value is called the steady state load, from which the steady state average die pressure P is defined as

$$P = \frac{L}{rA} .$$

The solution of any axi-symmetric problem of the type considered has as a desired end result the determination of P , since the mechanical design of forming apparatus is based largely on P .

1.2. Theoretical Considerations

Unlike their plane strain analogues, no exact mathematical solutions for P presently exist for axi-symmetric inverted extrusion or piercing. This difference in two apparently physically similar processes is due to a difference in the form of the governing differential equations.

Those of plane strain are hyperbolic¹ and, while they are not easily integrated analytically, their solutions may be obtained using a numerical or graphical procedure based on the method of characteristics.

The partial differential equations describing the axi-symmetric problem of piercing or extrusion are elliptic^{2,3} if the Mises yield criterion is used; as yet, no methods have been devised to integrate them or to obtain their solutions numerically. As their characteristics are imaginary the method of characteristics is not applicable.

CHAPTER 2

FORMULAS FOR THE PLANE STRAIN AND AXI-SYMMETRIC PROCESSES

Despite the mathematical difference in their governing equations, experiments have shown that for a given reduction the die pressures of plane strain and axi-symmetry are comparable.

2.1 Experimental Comparison of

Plane Strain and Axi-Symmetry

Purchase and Tupper⁴ have compared the results of their plane strain extrusions of lead with those of Pearson⁵, which were for the axi-symmetric inverted extrusion of lead. Plots of die pressure against reduction were almost identical in the range of reductions from 0.65 to 0.90. Johnston and Dodeja⁶ have, however, shown that the die pressures of plane strain inverted extrusion are always less than those of the axi-symmetric case, although the deviation decreased with increasing reduction. A possible explanation for the very close agreement found in the former case is that there was a fortuitous difference in the properties of the lead used by the investigators.

2.2 Empirical Relations for Axi-Symmetry

Johnson and Dodeja⁷ have suggested that the theoretically derivable relation

$$\frac{P}{2K} = \frac{a}{r} + \frac{b}{r} \ln \frac{1}{1-r} \quad \dots\dots\dots 2.1$$

for the plane strain inverted extrusion of an ideal non-hardening material be modified to suite the axi-symmetric

extrusion problem. K is the yield stress in pure shear and is equal to $Y/2$ if the Tresca yield criterion is used or $Y/\sqrt{3}$ if the Mises yield criterion is used. Y for the non-hardening material considered is the uni-axial yield stress as obtained from a compression test.

It follows from symmetry that if the container walls are smooth, and if the dead metal regions are the same, then the steady state die pressures of plane strain inverted extrusion are equal to those of plane strain piercing from the same reduction. Consequently Eq. 2.1. also applies to plane strain piercing.

Johnson and Dodeja⁸ suggested that an empirical relation, similar to Eq. 2.1, of the form

$$P = Y \left(\frac{c}{r} + \frac{d}{r} \ln \frac{1}{1-r} \right) \dots\dots\dots 2.2$$

should obtain for the axi-symmetric inverted extrusion of a non-hardening material. They assumed

$$P = Y \left(\frac{.8}{r} + \frac{1.5}{r} \ln \frac{1}{1-r} \right) \dots\dots\dots 2.3$$

$$0.5 \leq r \leq 0.94$$

to hold for the lubricated axi-symmetric inverted extrusion of a non-hardening material (and a work-hardening material by a method to be discussed later). The constants were deduced from the results of axi-symmetric inverted extrusion experiments on pure lead, which is effectively non-hardening at room temperature.

In contrast to the equations of the form 2.2, Hill⁹ has suggested a form of

$$P = \frac{BY}{r} \ln \frac{1}{1-r} \dots\dots\dots 2.4$$

to hold for the larger reductions of axi-symmetric inverted extrusion. Hill obtained a value of B of 1.45 which was substantiated by Pearson and Parkins.¹⁰ This last result is a

direct comparison of the actual extrusion pressures with the minimum ideal extrusion pressure of

$$P_i = \frac{Y}{r} \ln \frac{1}{1-r} . \quad \dots\dots\dots 2.5$$

B may be defined as the deformation efficiency by the formula

$$B = \frac{P_i}{P} . \quad \dots\dots\dots 2.6$$

One purpose of the experiments described in this thesis is to obtain a comparison of the axi-symmetric inverted extrusion and piercing pressures, and to obtain empirical relationships to compare with Eqs. 2.3 and 2.4 in order to test the general reproducibility of test results.

... ..

... ..

... ..

... ..

CHAPTER 3

USE OF AVERAGE YIELD STRESS FOR WORK-HARDENING MATERIALS

The experiments were performed using 0.06 percent tellurium lead in both the fully-hardened and annealed states, in order to determine the effect of the stress-strain relationship on the die pressures.

3.1. Explanation of Method of Average Yield Stress

The effects of work-hardening may be introduced into a study of these processes in a straight forward manner; the success of which, seems to vary greatly judging from the published reports. An explanation of the method is as follows.¹¹

Consider an axi-symmetric piercing or inverted extrusion proceeding in the steady state region. The extruded material is assumed to be isotropic and homogeneous; its yield stress $\bar{\sigma}$, for a particular element, being a function of the total plastic work per unit volume, W_p , performed on the element since the material was last in its annealed state. This may be expressed as

$$\bar{\sigma} = F(W_p). \quad \dots\dots\dots 3.1$$

W_p is given in the usual tensor notation by

$$W_p = \int \sigma_{ij} de_{ij}^p \quad \dots\dots\dots 3.2$$

where the integral is taken over the strain-path for the element considered.

Assuming that the Mises yield criterion is valid, then in the plastic

region for a particular element

$$\frac{\sigma'_{ij}\sigma'_{ij}}{2} = k^2 = \frac{\bar{\sigma}^2}{3} \quad \dots\dots\dots 3.3$$

where σ'_{ij} are the deviatoric components

of the stress tensor for the element considered. Equation 3.3 expanded in cylindrical polar coordinates, with the conventional notation, becomes for the axi-symmetric case

$$(\sigma_r - \sigma_\theta)^2 + (\sigma_r - \sigma_z)^2 + (\sigma_\theta - \sigma_z)^2 + 6\sigma_{rz}^2 = 2\bar{\sigma}^2 \quad \dots\dots\dots 3.4$$

Further, the generalized strain-increment for an element is defined as

$$d\bar{e}^P = +\sqrt{\frac{2}{3}} (de^P_{ij} de^P_{ij})^{1/2} \quad \dots\dots\dots 3.5$$

where de^P_{ij} is the deviator component of

the plastic strain tensor. Expanded in cylindrical polar coordinates, with conventional notation, Eq. 3.5 becomes for the axi-symmetric case

$$d\bar{e}^P = +\sqrt{\frac{2}{3}} \sqrt{\frac{(de^P_r - de^P_\theta)^2 + (de^P_r - de^P_z)^2 + (de^P_\theta - de^P_z)^2 + 3de^P_{rz}^2}{2}} \quad \dots\dots 3.6$$

It may be shown that

$$W_p = \int_0^{\bar{e}^P} \bar{\sigma} d\bar{e}^P \quad \dots\dots\dots 3.7$$

Equation 3.1 then becomes

$$\bar{\sigma} = F \left[\int_0^{\bar{e}^P} \bar{\sigma} d\bar{e}^P \right]$$

which reduces to

$$\bar{\sigma} = H \left(\int d\bar{e}^P \right), \quad \dots\dots\dots 3.8$$

so that $\bar{\sigma}$ is really a function of

$\int d\bar{e}^P$ if Mises yield criterion is used. In an uni-axial compression test of a rigid plastic $\int d\bar{e}^P$ reduces to the logarithmic strain.

With reference to Eq. 3.8 a metal is said to be fully-hardened

when

$$\frac{d\bar{\sigma}}{d\bar{e}^P} = 0.$$

The yield stress at which this occurs is termed the saturation stress.

Equation 3.7 indicates that the average work per unit volume of extruded material is given by

$$W = \frac{1}{V} \int_V \int_{\bar{e}^P} \bar{\sigma} d\bar{e}^P dV$$

$$= \text{Pr} \dots\dots\dots 3.9$$

where V is the volume extruded in a given time.

To obtain an analytical solution to Eq. 3.9 the relationship specified by Eq. 3.8 must be known for every element along its strain-path in the plastic region. The integral has yet to be solved analytically for non-trivial problems. It has, however, been solved numerically using data obtained by viscoplastic techniques. Thomsen¹² considered the axi-symmetric inverted extrusion of aluminum and, using the assumption that the stress-generalized strain relationship for each element was the same as that obtained from a uni-axial compression test, found P to be 95000 p.s.i as compared with the experimental value of 895000 p.s.i. This was for a reduction of 0.878.

If a non-hardening material is considered Eq. 3.9 reduces to

$$W = \frac{Y}{V} \int_V \int_{\bar{e}^P} d\bar{e}^P dV$$

which, upon assuming an average generalized strain-increment to apply to all elements, becomes

$$W = Y [\bar{e}^P]. \dots\dots\dots 3.10$$

$[\bar{e}^P]$ shall be termed the mean equivalent strain.

3.2 Computation of Average Stress

from the Stress-Strain Diagram

Equation 3.10 may be related to the stress-strain diagram for a non-hardening material on the hypothesis, that the amount of plastic work

required to produce a given $[\bar{\epsilon}^P]$ does not depend on the forming operation. Neglecting any initial rounding of the true stress-logarithmic strain diagram for the cold-worked tellurium lead (Fig. 14), then Eq. 3.10 may be considered as being equal to the area under the stress-strain diagram up to a logarithmic strain of $[\bar{\epsilon}^P]$.

If it is assumed, that the mean equivalent strain imparted to a material in a given forming operation is independent of the materials work-hardening characteristics, then r^P for the annealed material may be considered as the area under the true stress-logarithmic strain diagram up to a logarithmic strain of $[\bar{\epsilon}^P]$. $[\bar{\epsilon}^P]$ is evaluated from experimental results for the cold-worked (and supposedly non-hardening) material.

This method is equivalent to using an averaged yield stress, \bar{Y} , in Eq. 3.10 where \bar{Y} is the average yield stress over a logarithmic strain of $[\bar{\epsilon}^P]$ on the stress-strain diagram. Equation 3.10 may then be written more generally as

$$W = \bar{Y}[\bar{\epsilon}^P]. \quad \dots\dots\dots 3.10a$$

If the method is valid, it would be extremely useful because it provides a direct correlation between the stress-strain diagram for the material and the steady state forming pressures.

Thomsen and Frisch¹³ found, by visioplastic methods, that the flow patterns for the axi-symmetric inverted extrusion of aluminum and lead were very similar. Since, the aluminum was work-hardening and the lead was non-hardening, then their findings would tend to justify the assumption of a common $[\bar{\epsilon}^P]$.

3.3. Experimental Justification

for the Use of an Averaged Stress

The concept of an averaged yield stress was used by Johnson¹⁴ in the plane strain extrusion of lead, tellurium lead, and aluminum

with reported good results. Dodeja and Johnson¹⁵ used the same idea in studying the axi-symmetric inverted extrusion of lead, tellurium lead and super-pure aluminum with reductions of 0.75, 0.86, and 0.938. The results of the lead experiments (the lead was effectively non-hardening) were used to obtain the constants of Eq. 2.3. Then for any reduction the mean equivalent strain was found to be

$$[\bar{\epsilon}^P] = 0.8 + 1.5 \ln \frac{1}{1-r} . \quad \text{.....3.11}$$

Using a logarithmic strain obtained from Eq. 3.11 the maximum error between the experimental and calculated value of P_r for the aluminum was eight percent.

Haddow and Johnson¹⁶ applied the method of using an averaged yield stress to the axi-symmetric piercing of annealed 0.065 percent tellurium lead. The results presented give differences between the calculated P and the measured P which increased from ten percent to twenty percent over the range of reductions 0.55 to 0.80.

Due to the wide variation in the success of the application of the assumption of a common mean equivalent strain for materials with different hardening characteristics, in a given forming operation, it was desired to test its accuracy.

CHAPTER 4

DETERMINATION OF BOUNDS FOR THE FORMING LOADS

4.1. Concept of Bounds on P

A more theoretical approach to the determination of P is that of finding upper and lower bounds to P. This method is based on extremum principles due to Hill.¹⁷

The die pressure

$$P = \frac{Y}{r} \ln \frac{1}{1-r} \dots\dots\dots 4.1$$

would be obtained in an ideal extrusion of a non-hardening material, where ideal means that there is no redundant shearing. This pressure is a lower bound for either the axi-symmetric inverted extrusion or piercing problem. However, the strain-path of an element in homogeneous deformation is very different from that of the actual process. This indicates that Eq.4.1 is not a close lower bound. The idea of the upper and lower bound is to obtain the closest bound.

4.2 Application of Bounding Techniques

to Piercing

Haddow and Johnson¹⁸ have presented their minimum upper bounds for axi-symmetric piercing with flat lubricated and flat rough punches in comparison with experimental results. A rough punch is one which will allow the working metal to develop its full shear strength across the punch face. The upper bound for the smooth punch bounds the experimental results very closely but the bound for a rough punch is about 25 percent above the experimental results.

Haddow and Johnson¹⁹ have also obtained a lower bound to the axi-symmetric piercing of a non-hardening rigid plastic. This bound does not depend on an extremum principle because it is based on homogeneous deformation which must be more efficient than any other strain-path. A graphical presentation of their solution is shown in Fig. 16, and is compared with the results obtained in this investigation for piercing cold-worked 0.06 tellurium lead.

4.3. Neglect of Friction in Piercing

Most investigators (e.g.) Haddow and Johnson²⁰ have usually assumed that during a piercing test the drag between the pierced material and the container wall was small (with proper lubrication) and had negligible effect on P . The basis of this assumption no doubt being that steady state die pressures were achieved. If the drag was of importance, then it should conceivably increase during a test and therefore result in an increasing P . Despite these findings, which indicate that for a lubricated sliding fit the drag is small, it was felt to be of interest to determine the range of magnitudes of the drag force and also its variation with r .

CHAPTER 5

APPARATUS AND MATERIAL

The essential features of the apparatus used in these experiments are shown in Figs. 1 and 2.

The container (medium carbon steel) had a honed bore of 1.753 inches and was used for both the inverted extrusion and piercing experiments.

Loads were applied using a 200,000 pound Baldwin testing machine.

The die travel was obtained from a two inch travel dial gage which measured the movement of the hydraulic ram (see Fig.13).

5.1. Inverted Extrusion Apparatus

Features peculiar to the inverted extrusion apparatus were the dies and the load sleeves.

The dies were of Keewatin steel, 0.5 inches thick, 1.752 inches in outer diameter, and had an included angle of 25 degrees at the aperture. Faces in contact with the container bore and with the billet were lapped.

Load sleeves were made to cover the complete range of die sizes; the external diameters were constant with the internal diameters being appropriately varied.

5.2. Piercing Apparatus

The piercing apparatus, as shown in Fig. 2, was more complex than that for the extrusion experiments.

Instead of using one piece punches, as Haddow and Johnson²¹

did, it was decided that the lathe work could be reduced by using a common loading sleeve for all the punches. This necessitated the provision of a centering sleeve and a centering bushing, shown in Fig. 2, to keep the stem and punch in axial alignment with each other and with the cylinder. A ball-bearing connection would have been desirable between the stem and punch to ensure axial application of the load, but this was not provided.

Generally, in piercing experiments, the container and closure plate are bolted together. It was desired, however, in these experiments to measure the drag of the pierced material on the container. This was done by attaching three beryllium-copper tensometer strips, which were spaced at 120 degree intervals about the container. Their extension underload, which is directly related to the load, was measured using strain gages. A swivel mounting, as shown in Fig. 2, was used to ensure purely tensile loading in the strips. The swivels were made of $3/8$ inch diameter brass stock and were designed on the assumption that the maximum friction loading would not exceed 600 pounds. This proved much too conservative an estimate and as such the swivels were under-designed. Protective casings were provided for the tensometers.

Three centering pins were provided to prevent rotation of the container about its vertical axis.

The punches were made of Keewatin steel with the faces being hardened, ground, and lapped. A 0.5 inch threaded hole was provided in the ends of the larger punches to facilitate their removal from the pierced material.

5.3. Billet Forming Apparatus

Billets were formed using the apparatus shown in Fig. 3.

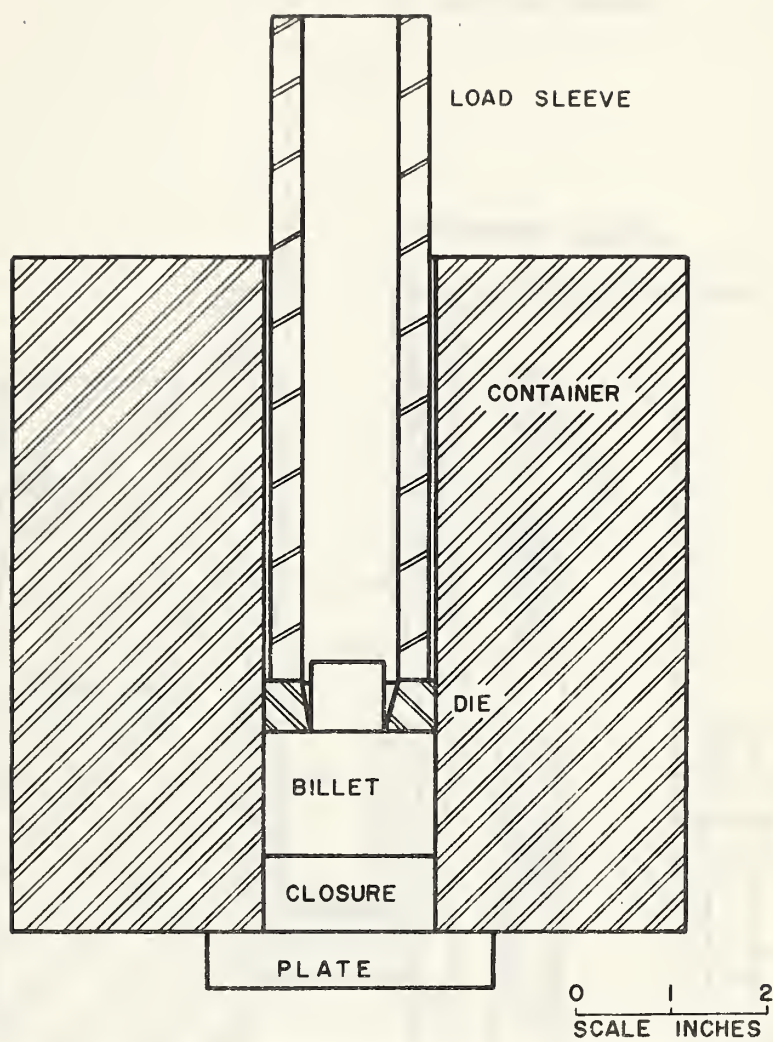


FIGURE 1. INVERTED EXTRUSION APPARATUS

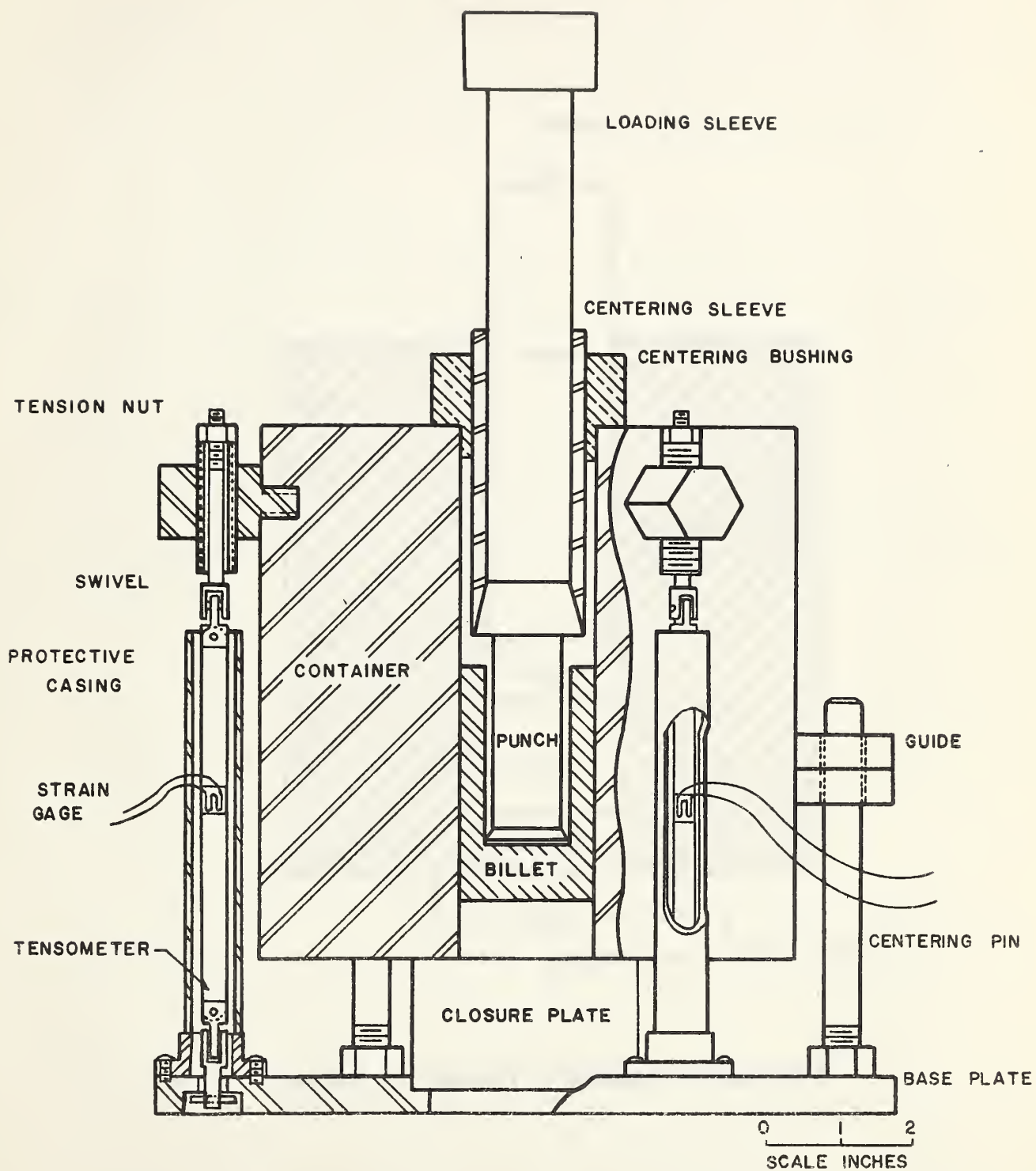


FIGURE 2. PIERCING APPARATUS

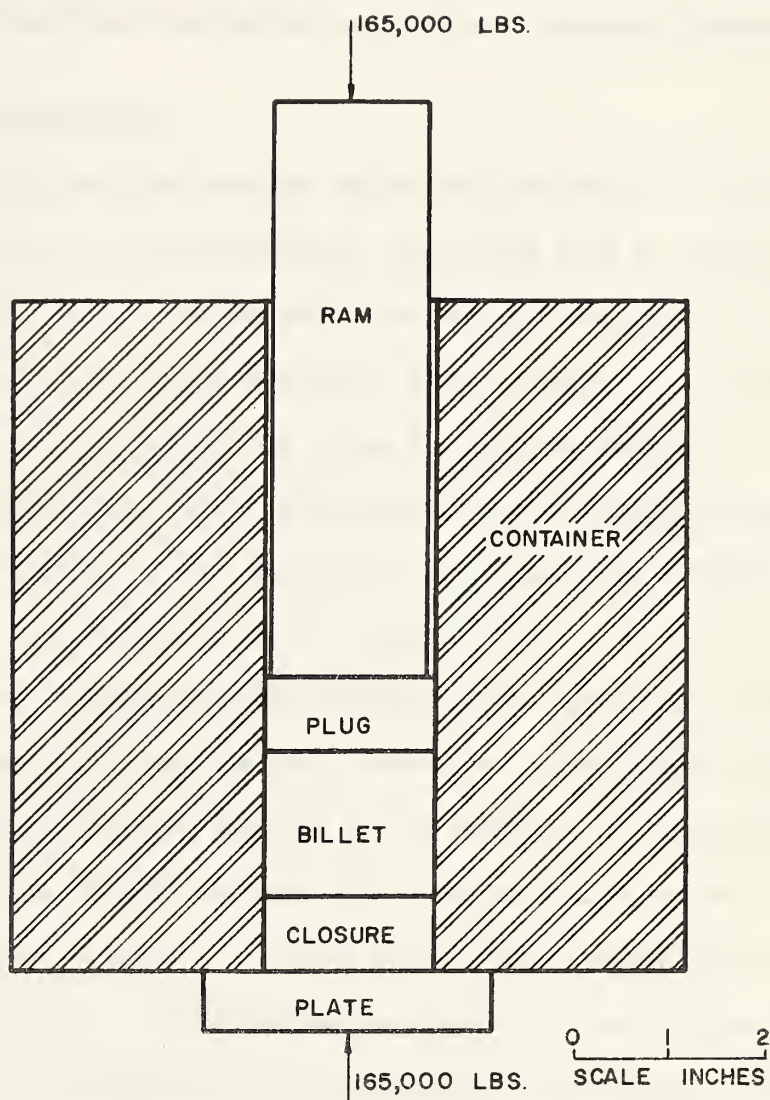


FIGURE 3. BILLET FORMING APPARATUS

The cylinder was similar to that used for the extrusion experiments except that it had a honed bore of 1.751 inches.

A problem encountered in the billet formation was plastic buckling of the 1.7 inch diameter by 6 inch long ram. This effect was minimized by ensuring that the compression platen on the cross-head was level and that the platen and ram were axially aligned.

5.4. Billet Preparation

Initially the 0.06 percent tellurium lead was in the form of cast billets, 4 x 4 x 17 inches long. The first step in the preparation of the specimens was to saw the castings into 1.25 x 1.25 x 2.25 inch long blocks which were filed smooth and then cold-worked, at room temperature, until the final dimensions were approximately 1 x 1 x 3.5 inches long. This cold-working was intended to break up the cast grain structure, and probably did so since the recrystallisation temperature of tellurium lead is near 120°C.²²

The final forming operation employed the apparatus shown in Fig. 3. The bore was lubricated with vaseline. Although a compressive stress of 65,000 p.s.i. was applied to the billets, it was necessary to put some of the billets through this last operation twice to obtain a suitable surface finish. The final billet size was approximately 1.5 inches in length by 1.752 inches in diameter. The billets formed in this way were a sliding fit in the lubricated extrusion container.

A sufficient number of work-hardened billets for a complete set of tests were made at one time. They were kept refrigerated at 30-40°F. until used. Hofmann and Hanemann²² observed age-hardening in 0.1 percent tellurium lead which had been cold-worked, but checks of the refrigerated specimens hardness numbers did not show any noticeable variation from their original values.

Annealed billets were made by annealing the work-hardened specimens for two hours at 240°C . The Vickers diamond hardness number of the annealed material was approximately 4.4 as compared to 8.7 for the work-hardened material. A load of 500 grams was used for the hardness tests.

The hardness numbers varied by as much as five percent across a billet face. This was believed to be due to the fact that a Tukon hardness tester was used to take hardness measurements on unprepared billet surfaces. Since the Tukon hardness tester is a micro-hardness tester the surfaces should have been prepared, but this was not done.

To check for dead metal in the extrusion experiments, one billet for each reduction had concentric grooves, 0.01 inches deep and spaced at 0.1 inches, inscribed on one end. Yellow crayon was rubbed into these grooves. This colouring was trapped when the die pressure closed the grooves and thus provided a clear record of the groove. If an extrusion experiment using one of these billets was halted in the steady state region, then, the absence of dead metal was indicated by an inward movement of the concentric grooves.

If a milling machine had been available the above method of checking for dead metal would have been replaced by grid deformation experiments on sectioned billets. This method has the advantage of indicating both the presence of dead metal and the shape of its boundary.

CHAPTER 6

STRESS-STRAIN COMPRESSION TEST

6.1. Discussion of the Compression Test

The purpose of a compression test is to obtain the relationship between the uni-axial yield stress and the logarithmic strain under conditions of homogeneous deformation.

Logarithmic strain is chosen in preference to conventional engineering strain, since, for large plastic deformations the current configuration and not the original configuration is of importance. Further justification for using logarithmic strain is that the plastic work per unit volume in the uni-axial compression of an elastic-plastic material is given by²³

$$w_p = \int_l^{l_0} \bar{\sigma} d\left(\ln \frac{l_0}{l} - \frac{\bar{\sigma}}{E}\right)$$

where l_0 is the initial length and l is the current length of the test specimen. $\bar{\sigma}$ is the current yield stress. The above integral is equal to the area under the true stress-logarithmic plastic strain curve.

Approximately homogeneous deformation may be obtained by using lubricated compression platens, with any barreling of the specimen being frequently removed by turning the specimen down on a lathe.

It is desirable to keep the height to width ratio of a cylindrical billet between 1.5 and 1 to avoid the possibilities of plastic buckling or non-uniform deformation modes. Towards the end of a compression test it is not feasible to keep the height greater than the diameter; in fact, the diameter may become as large as fifteen times the height (Johnson¹⁴). The friction drag acting on the compression

platens may then have a considerable effect on the yield stress, but may be corrected for by a formula due to Siebel²⁴, which states that

$$\bar{\sigma} = \frac{P}{\left(1 + \frac{2u}{3} \frac{a}{h}\right)}$$

P is the applied average pressure, $2 \frac{a}{h}$ the diameter to height ratio, u the coefficient of friction, and $\bar{\sigma}$ the corrected yield stress. In his paper Johnson does not state whether this correction was applied.

6.2. Compression Test Procedure

The specimens, originally about 1.5 inches in height and 1.0 inches in diameter, were loaded in increments using the sub-press shown in Fig. 4.

A ball-bearing support was used to transfer the load from the load stem to the sleeve. The sleeve was a close fit in the container but was so designed that the load was carried by a reduced section, hence there was no tendency for the sleeve and container to bind due to a Poissons expansion effect on the sleeve.

The platens were made of hardened Keewatin steel and were lapped to a smooth finish. They were re-lubricated after each increment of loading. It should be noted that excess lubricant had a tendency to slightly pit the surface of the specimen.

For a work-hardened specimen a single stage of compression consisted of lubricating the platens, mounting the specimens in the sub-press, and then loading the specimen to a load about 200 pounds above that of the previous stage. The load was then immediately released. A micrometer was used to measure the current length of the specimen from which it was possible to compute the average cross-sectional area and hence the current yield stress. These stages were repeated until a trace of barreling appeared. The diameter of the

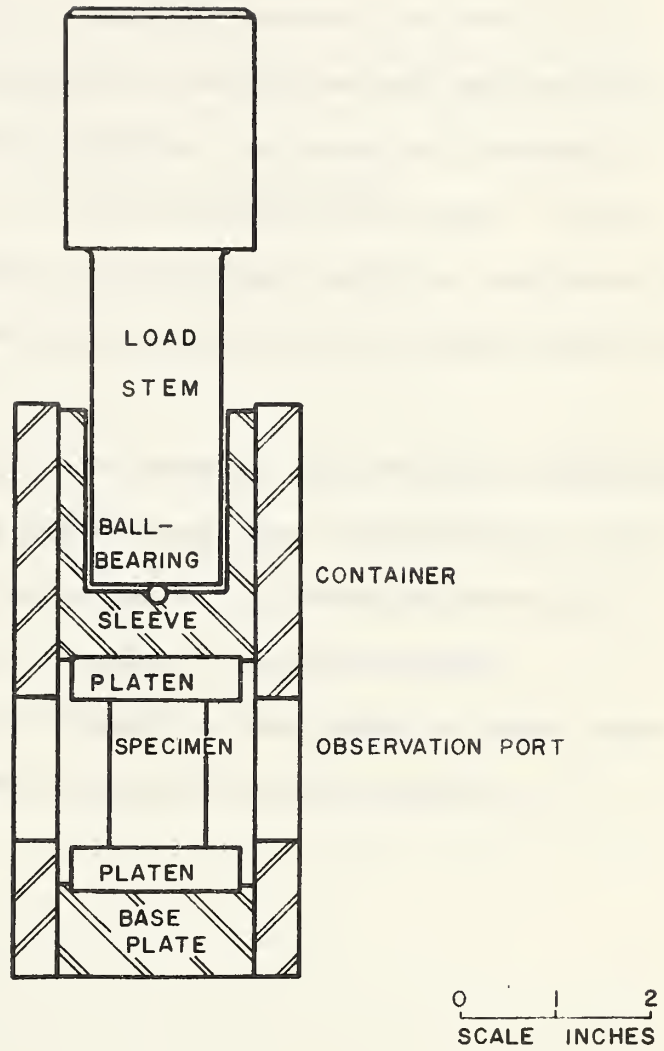


FIGURE 4. COMPRESSION SUB-PRESS

specimen was then reduced on a lathe, with sufficient coolant being supplied to maintain the specimen at room temperature. Figure 14 indicates the number of times a billet with original dimensions of 1.488 inches in height and 0.959 inches in diameter was machined during a test.

The only difference in procedure between the tests on the work-hardened and on the annealed tellurium lead was that for the former material, after each machining, the stress was increased in many steps (see Fig. 14) up to the previous yield stress. For the annealed material the first load, after each machining, was chosen to produce a stress within several hundred pounds per square inch of the last yield stress.

In both cases the elastic component of strain was automatically neglected by measuring the unloaded specimen. Unfortunately, the method of measurement was not sufficiently refined to detect any difference in the length of a loaded or unloaded specimen.

The ratio of average diameter to the height was never large compared with unity so Siebels correction was not applied.

CHAPTER 7

EXPERIMENTAL PROCEDURE

All the tests were carried out at a tool speed of 0.002 inches per second. Vaseline was used to lubricate the container bore and the die faces.

Before the dial gage, which was used to measure die travel, was set in position, the slack was taken out of the system by applying a load of approximately 100 pounds to the specimen.

7.1. Experimental Procedure - Piercing

After the slack had been taken out of the system a tension of about 25 pounds was applied to each tensometer strip. This was done by advancing the tension nuts shown in Fig. 2. Zero readings for the strain gages were then noted and the actual test was commenced. Numerous readings of die travel and ram loading were taken during a test. Readings of the strain indicator were also noted.

At the end of a test the billet was pushed from the container by supporting the latter and using the testing machine to provide the load. This load was less than the maximum recorded friction loading on the tensometers; its value was not recorded.

Removal of the punches from the worked specimens proved to be difficult for reductions of 0.5 and over. This was probably due to two factors. Namely, the pierced annulus was subject to elastic recovery and also the plastic region might have extended back past the punch face. To facilitate the withdrawal of the punch, the billet was held in a jig and impact loading was applied to the punch through a bolt screwed into the punch end. This method was rather clumsy and ruined the interior finish of the billet.

A problem encountered with the piercing apparatus was that the punch wandered for the 0.9 reduction. This was believed to be due to a slight eccentricity in the point of application of the load to the punch. The defect could probably have been corrected had a ball-bearing method of load application to the punch been provided. This however was not done and therefore no piercing results for this reduction were recorded.

7.2. Experimental Procedure - Inverted Extrusion

The procedure in an inverted extrusion test was the same as that for a piercing test, except that no readings were taken on the tensometers.

Extrusion tests using the billets with rings inscribed on one end were stopped in the steady state region so a check could be made for dead metal. The presence of the grooves did not appear to effect the ram load; indeed, no effect would be expected for completely dead metal.

Flashed metal between the extrusion die and the container was negligible.

For reductions greater than 0.6 the dies could not be removed by hand. This difficulty was overcome by sawing through the extruded metal immediately beside the die and then slipping the die off the severed end.

CHAPTER 8

EXPERIMENTAL RESULTS AND DISCUSSION

8.1. Autographic Diagrams

Typical autographic diagrams are shown in Figs. 5, 6, 7, and 8. They were plotted in the form of die pressure against the ratio of die travel to billet height. The steady state die pressures were obtained from plots such as these.

The steady state pressures, P , for the inverted extrusion of annealed tellurium lead were reproducible to within 1.5 percent of the mean.

Definite steady states did not occur in all cases for the extrusion of cold-worked tellurium lead. For reductions of 0.5 and above the working material seemed to undergo a gradual softening before a definite unsteady state set in. This could be due to the temperature rise associated with the process being large enough to cause a small amount of annealing.

Clearly defined steady state pressures were observed for the piercing experiments on the annealed material; this was also the case to a lesser extent for the piercing of cold-worked tellurium lead. The gradual softening effect, which was quite noticeable in the extrusion of the cold-worked material, was not so evident for the piercing experiments on the same material.

The results for cold-worked extrusions and piercings were reproducible to within three percent of the mean.

A feature peculiar to the autographic diagrams for the annealed material was the pronounced peak; it was particularly noticeable in the

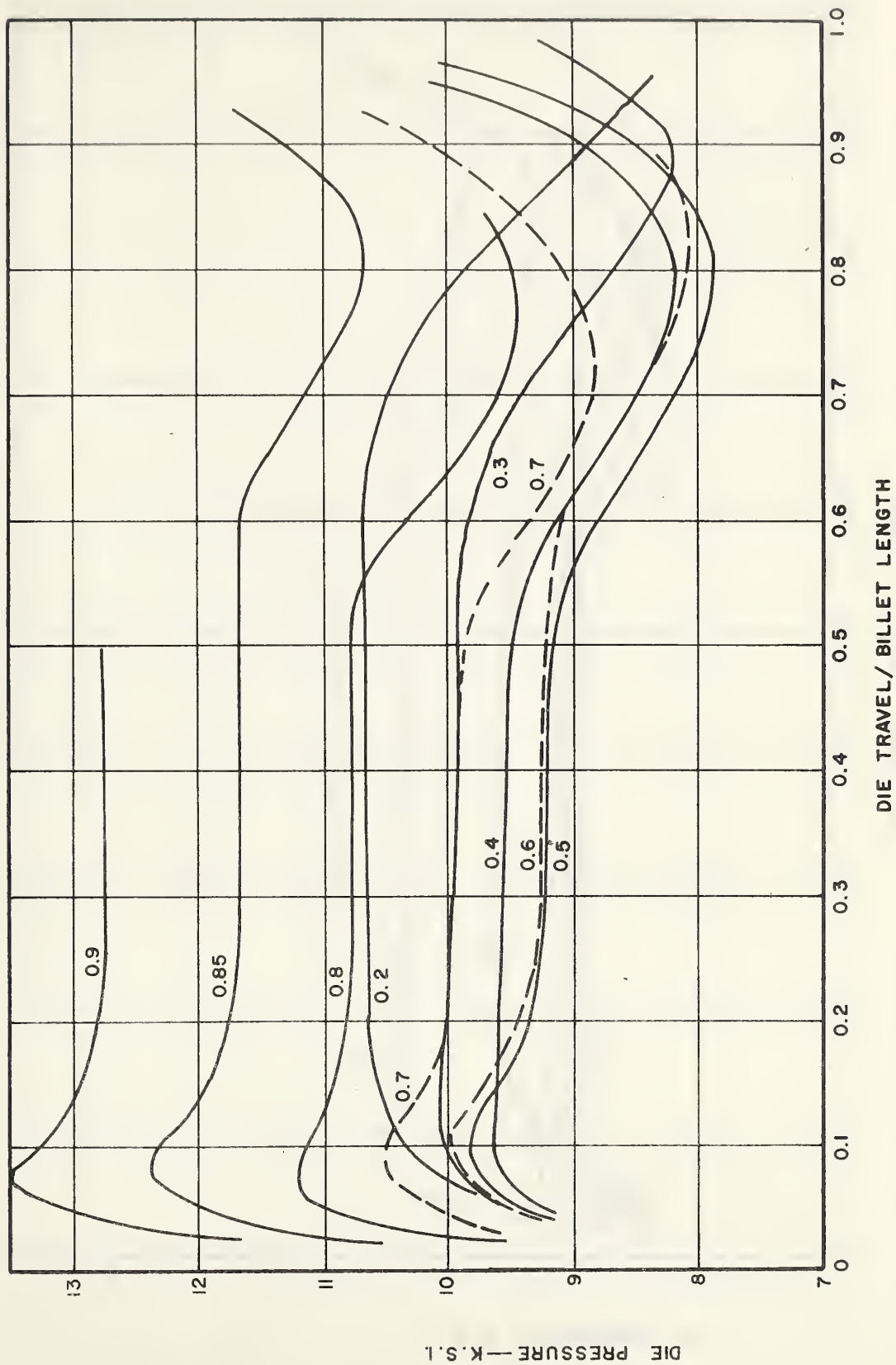


FIGURE 5. AUTOGRAPHIC DIAGRAMS FOR INVERTED EXTRUSION OF ANNEALED TELLURIUM LEAD

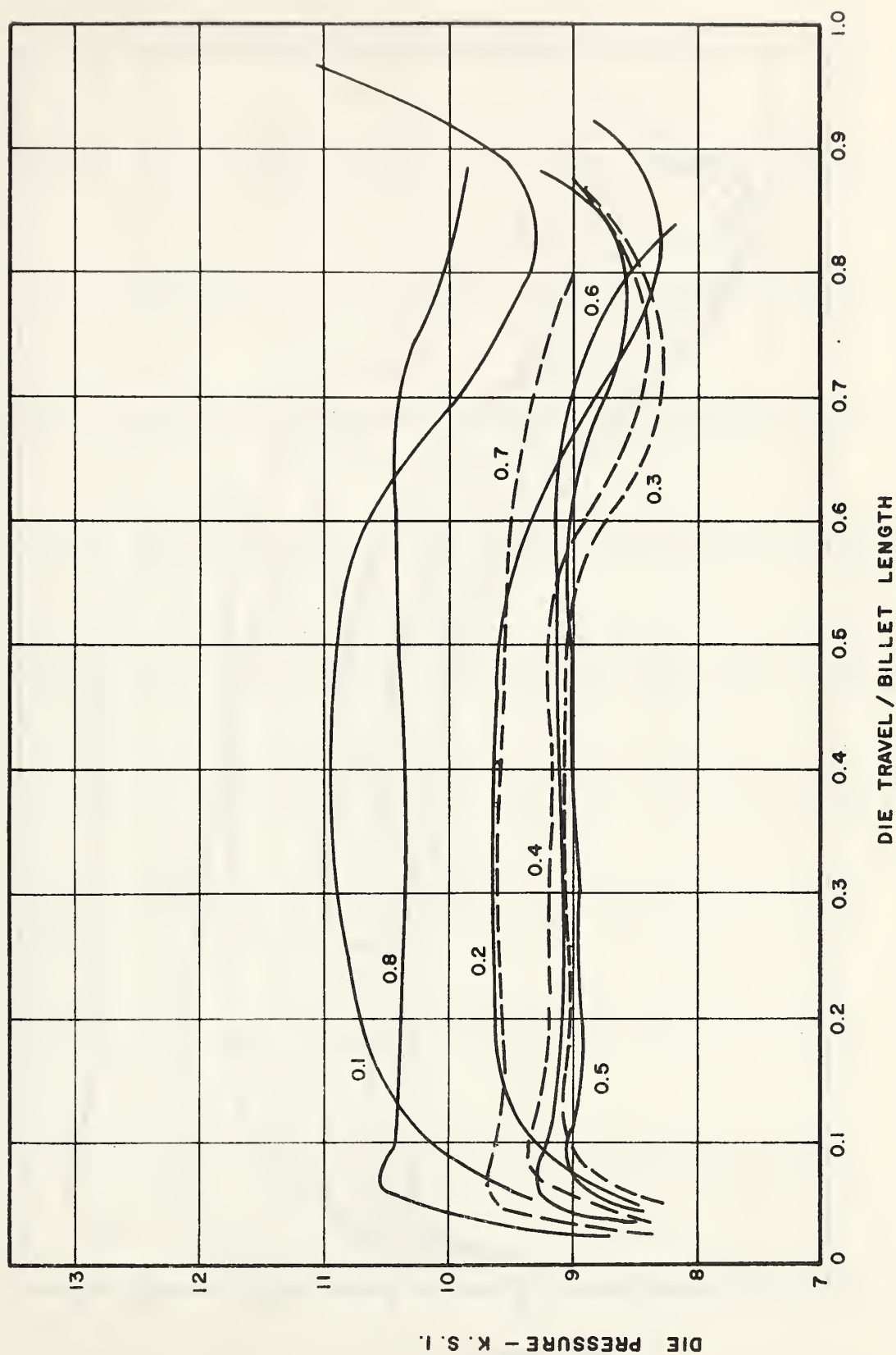


FIGURE 6. AUTOGRAPHIC DIAGRAMS FOR PIERCING OF ANNEALED TELLURIUM LEAD.

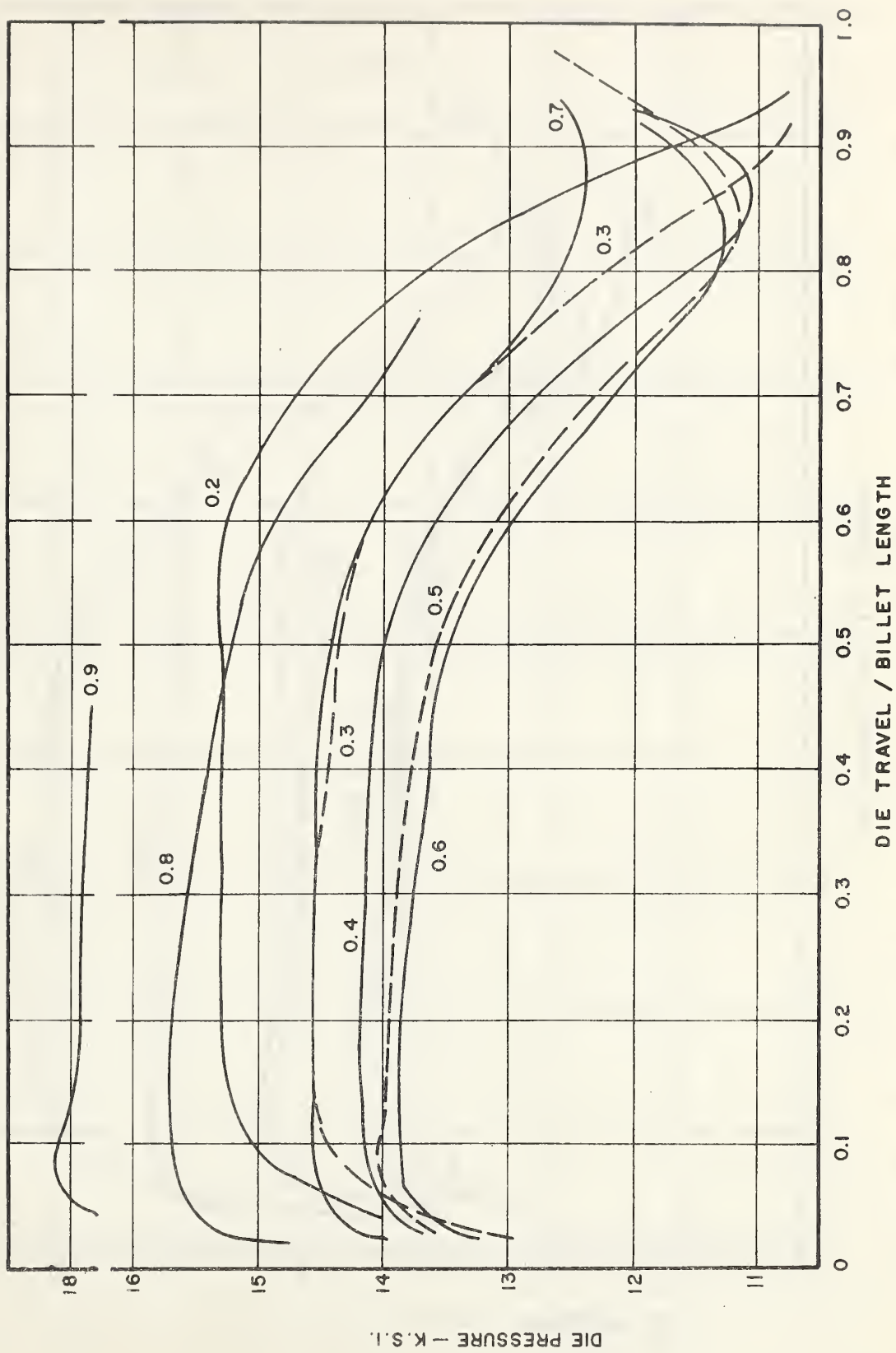


FIGURE 7. AUTOGRAPHIC DIAGRAMS FOR INVERTED EXTRUSION OF FULLY-HARDENED TELLURIUM LEAD

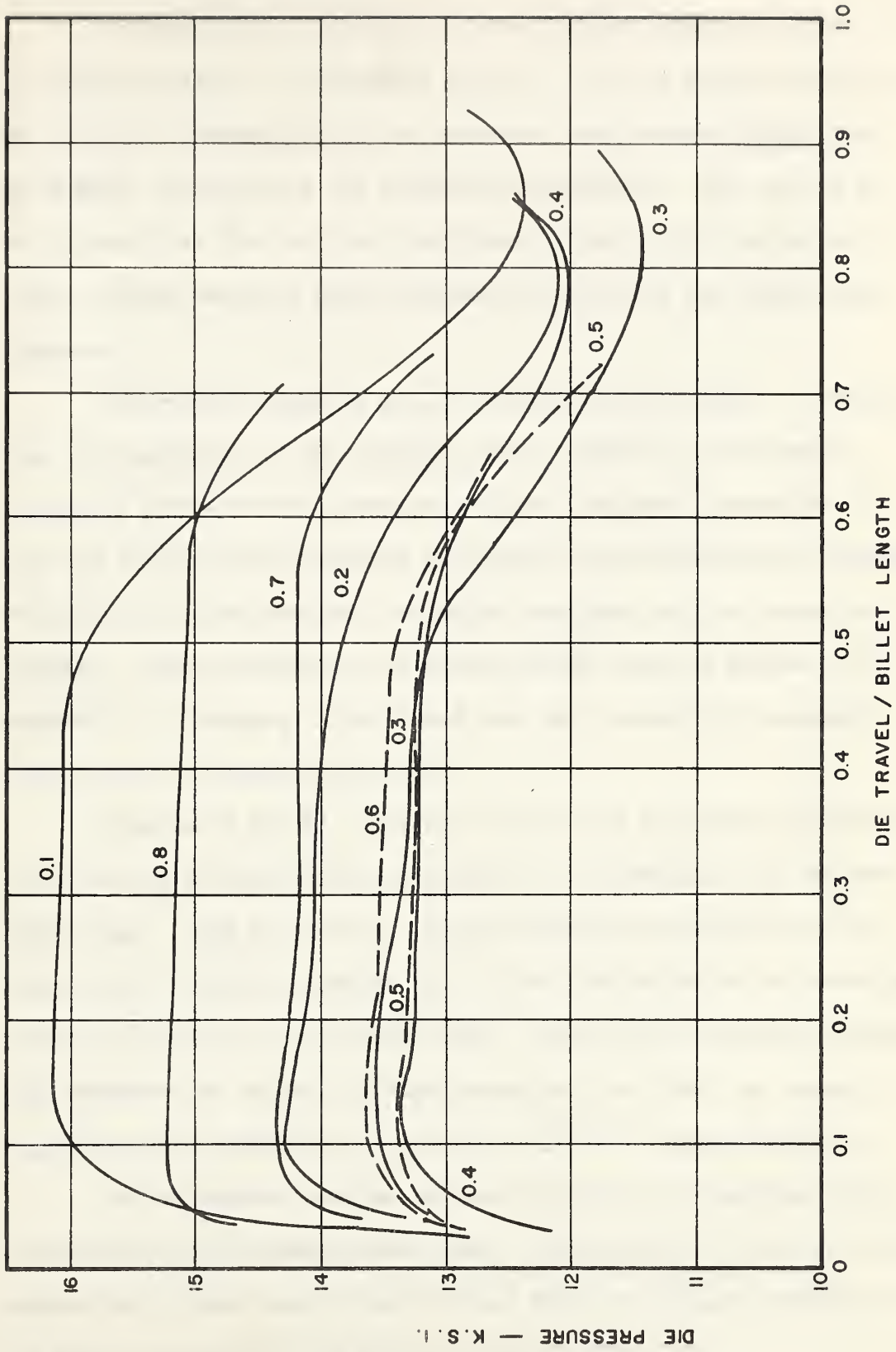


FIGURE 8. AUTOGRAPHIC DIAGRAMS FOR PIERCING OF FULLY-HARDENED TELLURIUM LEAD

large reductions by extrusion.

To examine the initiation of the unsteady state the ratio t/d was plotted against r as shown in Fig. 9. D is the punch diameter in the piercing experiments and the container bore diameter minus the die orifice diameter for the extrusion experiments. The value t is the distance the die was from the billet bottom on the initiation of a well defined unsteady state and was obtained from the autographic diagrams.

The results shown in Fig. 9, although very erratic, indicate that the initiation of the unsteady state depends on the physical properties of the working metal as well as the actual reduction. For both the piercing and extrusion experiments the unsteady state commenced earlier with the cold-worked tellurium lead than with the annealed material. These results are in contrast with those of Haddow and Johnson²⁵ for piercing. They found that the instability commenced earlier with the annealed material.

Figures 10 and 11 illustrate the cavity formations characteristic of the extrusion and piercing processes if a lubricated flat closure plate (Figs. 1 and 2) is used. These cavities are initiated at the start of the unsteady state as this is the time at which the advancing plastic region meets the closure plate. That the die pressure should then decrease may be seen by considering the fact that the energy expenditure for advancing the plastic field is no longer required.

The extrusion experiments using billets with inscribed grids were halted in the steady state region. They indicated that dead metal existed for r less than 0.5 but did not exist for larger values of r . The inward movement of the grids is shown in Fig. 12.

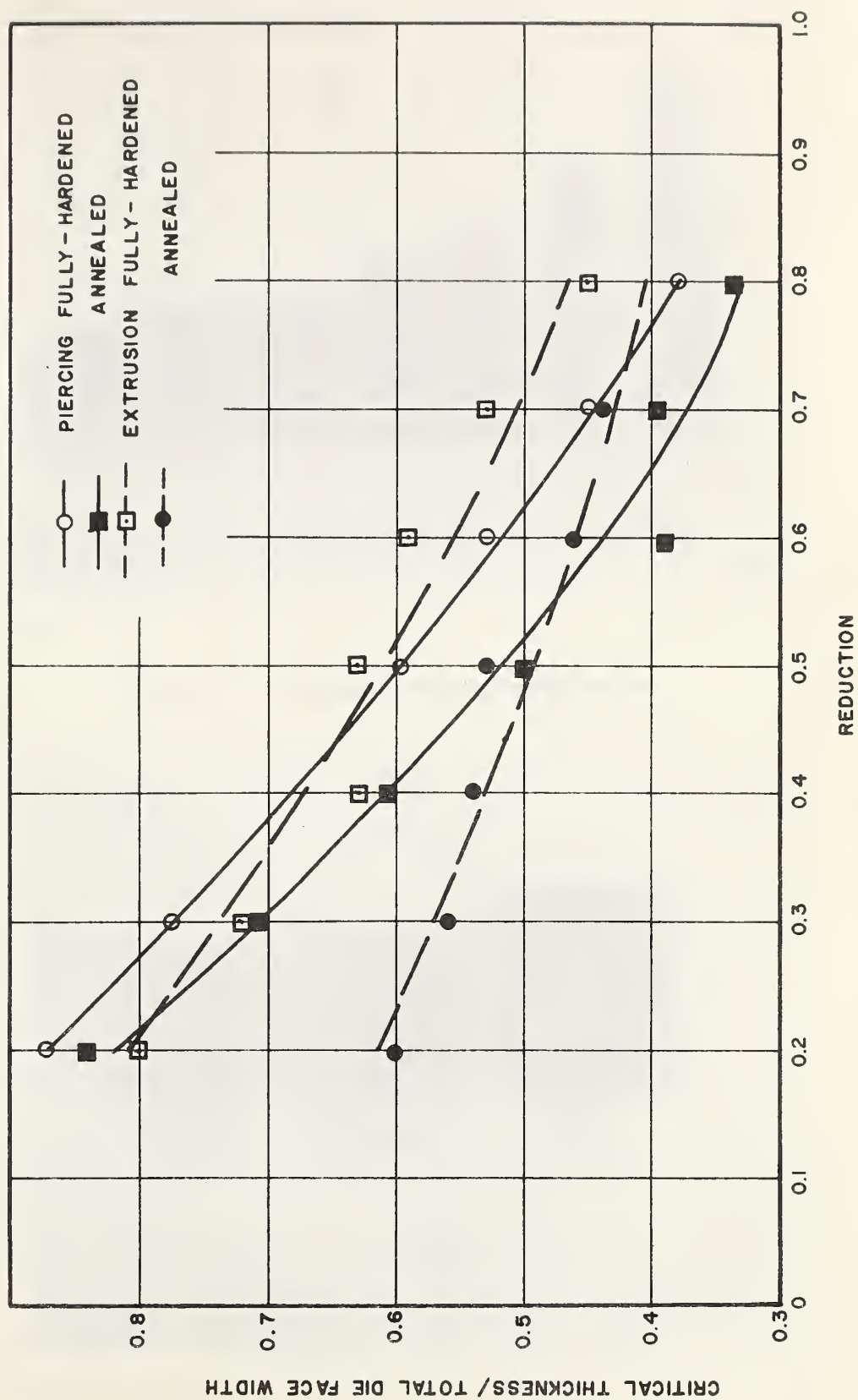


FIGURE 9. INITIATION OF UNSTEADY STATE



Figure 10. Cavity Formation---Extrusion

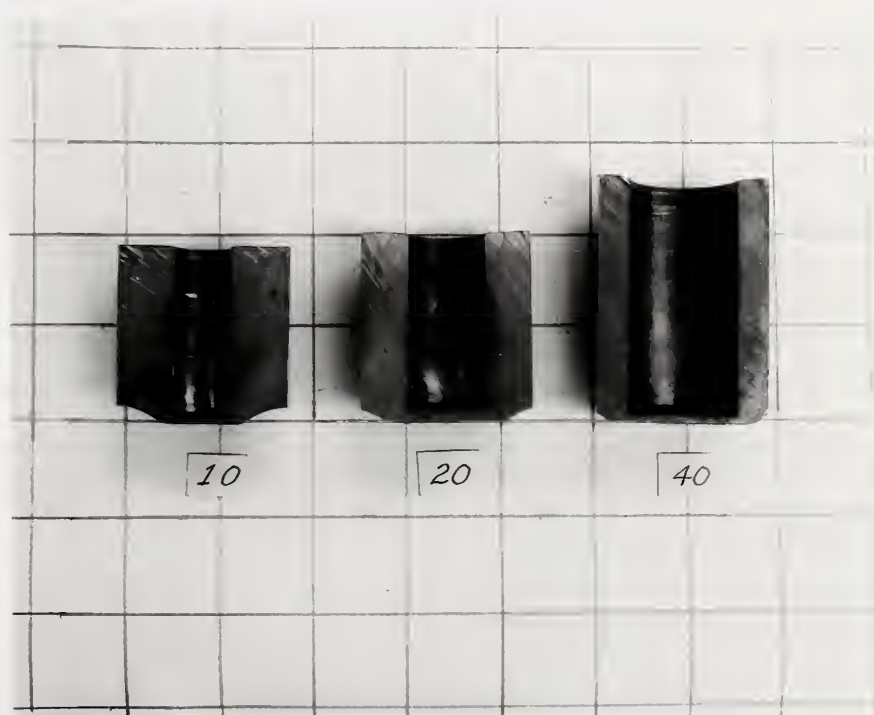


Figure 11. Cavity Formation---Piercing

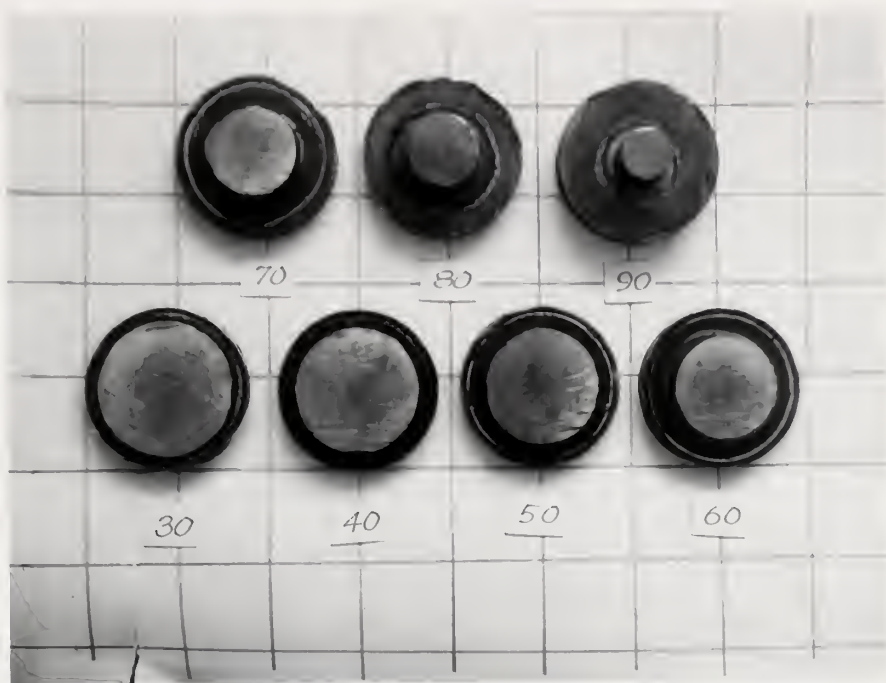


Figure 12. Photograph of Grid Movement in Check for Dead Metal---Extrusion

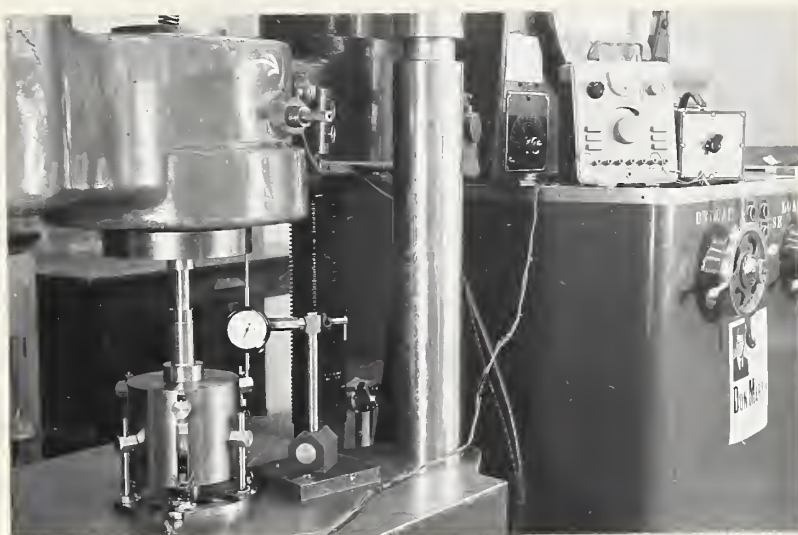


Figure 13. Piercing Apparatus in Place on Baldwin Testing Machine

8.2. Friction Results

In the piercing tests little or no friction drag was recorded until near the end of the steady state period, at which time the measured friction loading rose rapidly. This indicated that up to this point the friction drag between the lower part of the billet and the container plus the weight of the container was greater than the drag between the moving pierced material and the container. It does not indicate that up to this point there was no friction drag on the pierced annulus.

For the smaller reductions it was not possible to obtain a complete set of friction readings for the three tensometers until the rapid variation in the measured load ceased. This occurred near the minimum load point of the unsteady state region, at which time the measured friction loading reached a maximum and nearly constant value. This would indicate the need for an automatic device to record the friction variation continuously.

For the large reductions the tests were discontinued before the maximum friction point was reached, as is evident from the autographic diagrams in Figs. 6 and 8. This was done because the friction load on the tensometers had attained a value of 600 pounds, which was considered to be near the failure load of the swivels.

Since readings could be obtained only at the minimum point of the unsteady state region, it was not possible to apply any correction to the steady state die pressures. In spite of the friction effects, Figs. 6 and 8 indicate that a steady state load was attained. An exception was the 0.8 reduction of annealed tellurium lead, which had a well defined rise in steady state pressure.

Sample values of the measured maximum friction drag gave

added die pressures of 80, 150, 240, 275, and 550 p.s.i. for reductions of 0.1, 0.2, 0.3, 0.4, and 0.5. These values were not reproducible and any deviation in billet diameter seemed to effect the measured frictional drag by a considerable amount.

8.3. Stress-Strain Diagrams

True stress- logarithmic strain diagrams for both the annealed and the work-hardened tellurium lead are shown in Fig. 14.

The compression tests for the work-hardened material were terminated after a logarithmic strain of 1.2 as a well defined saturation stress had been attained.

Each stage of the reloading was plotted for the work-hardened material. It is noted that, for each reloading, there was a considerable amount of plastic strain before the yield stress attained its saturation value of 4050 p.s.i.

The stress-strain diagram for the annealed material is of interest. It would seem that upon sufficient plastic working the material should attain a maximum yield stress near that possessed by the original work-hardened material. However, after a logarithmic strain of about 1.0 the work-hardening rate became negligible and the yield stress attained an approximately constant value of 3250 p.s.i. as compared to 4050 p.s.i. for the work-hardened material. The compression tests on the annealed tellurium lead were terminated after a logarithmic strain of 1.9 as the specimens were becoming very small. Presumably, additional plastic work would tend to increase the yield stress, but this was neglected for the purposes of computing an average yield stress.

A possible explanation for the low rate of hardening exhibited by the annealed tellurium lead is that the material had a large grain size. Loizou and Sims²⁶ found that a very large grain size had a marked

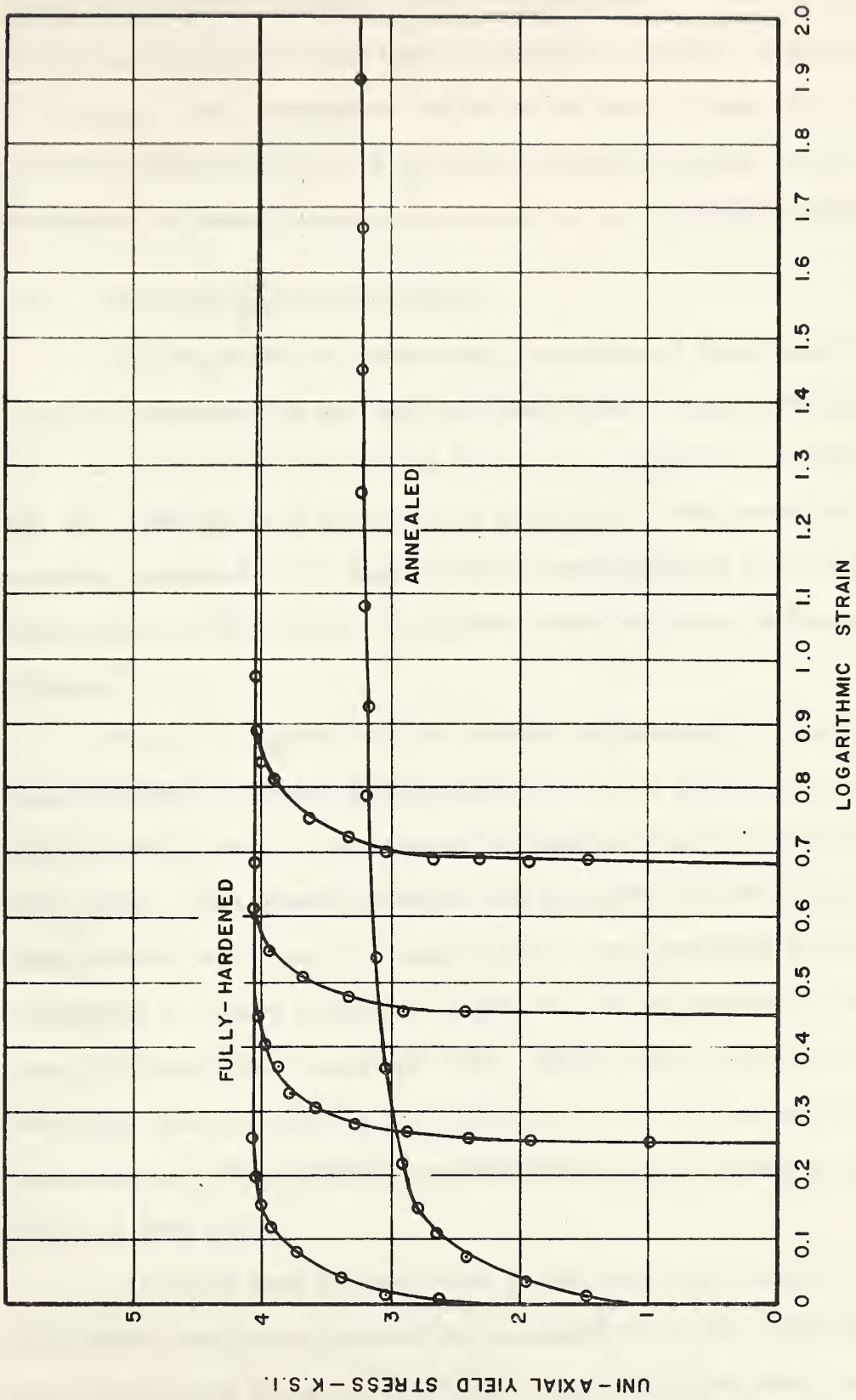


FIGURE 14. STRESS-STRAIN DIAGRAMS FOR TELLURIUM LEAD.

effect on the yield stress of pure annealed lead. A check for large grain size was made by examining a chemically polished cross-section of a billet. The examination failed to indicate a large grain size. This was attributed to the fact that the chemical polish had not been sufficient to remove the disturbed metal on the sectioned surface.

8.4. Pressure-Reduction Diagrams

The dependent and independent variables of these experiments were the die pressures and the area reductions. The experimentally determined relationships between P and r are presented in Figs. 15 and 16. Also shown in Fig. 16 is a theoretical lower bound to the piercing pressures for a rigid-plastic, non-hardening solid with a yield point of 4050 p.s.i. This lower bound is due to Haddow and Johnson.¹⁹

The P - r diagrams for the inverted extrusions of annealed and fully-hardened tellurium lead are similar. They both have well defined minimum points near a reduction of 0.5 and are fairly symmetrical about this point. This symmetry feature can be shown, theoretically, for the plane strain extrusion of a rigid-plastic, non-hardening solid and it is reasonable to expect a similar effect for the axi-symmetric process using fully-hardened tellurium lead. That it also applies to the annealed tellurium lead is probably due to the fact that this material closely approximates a rigid-plastic, non-hardening solid possessing a yield point of 3250 p.s.i.

It would seem reasonable to expect that the ordinates of the cold-worked tellurium lead and the annealed tellurium lead P - r diagrams should be in the ratio of 4050/3250. This is not the case; in fact, the ordinates differ by an approximately constant value of 4250 p.s.i.

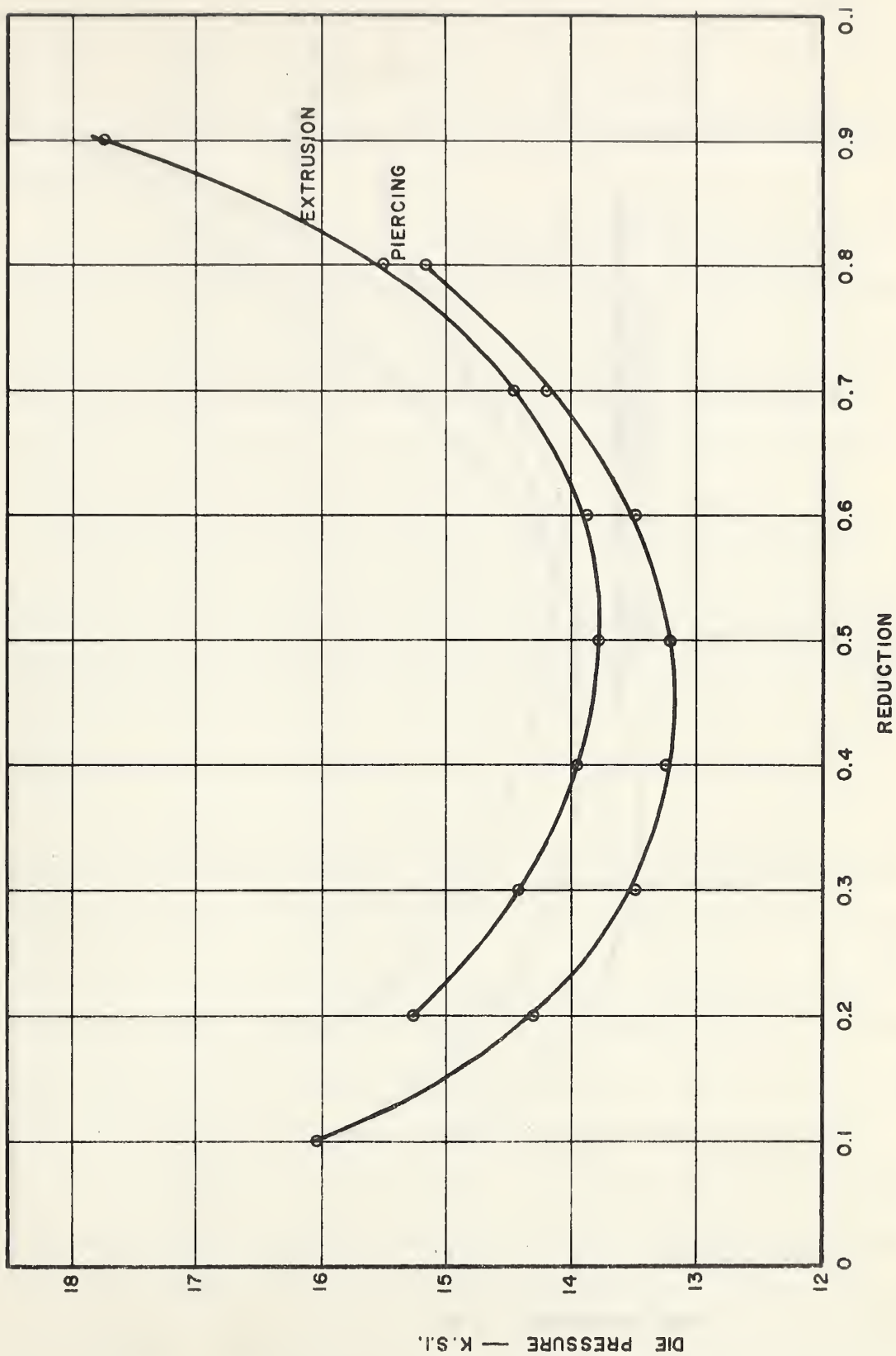


FIGURE 15. PRESSURE-REDUCTION DIAGRAMS FOR FULLY-HARDENED TELLURIUM LEAD

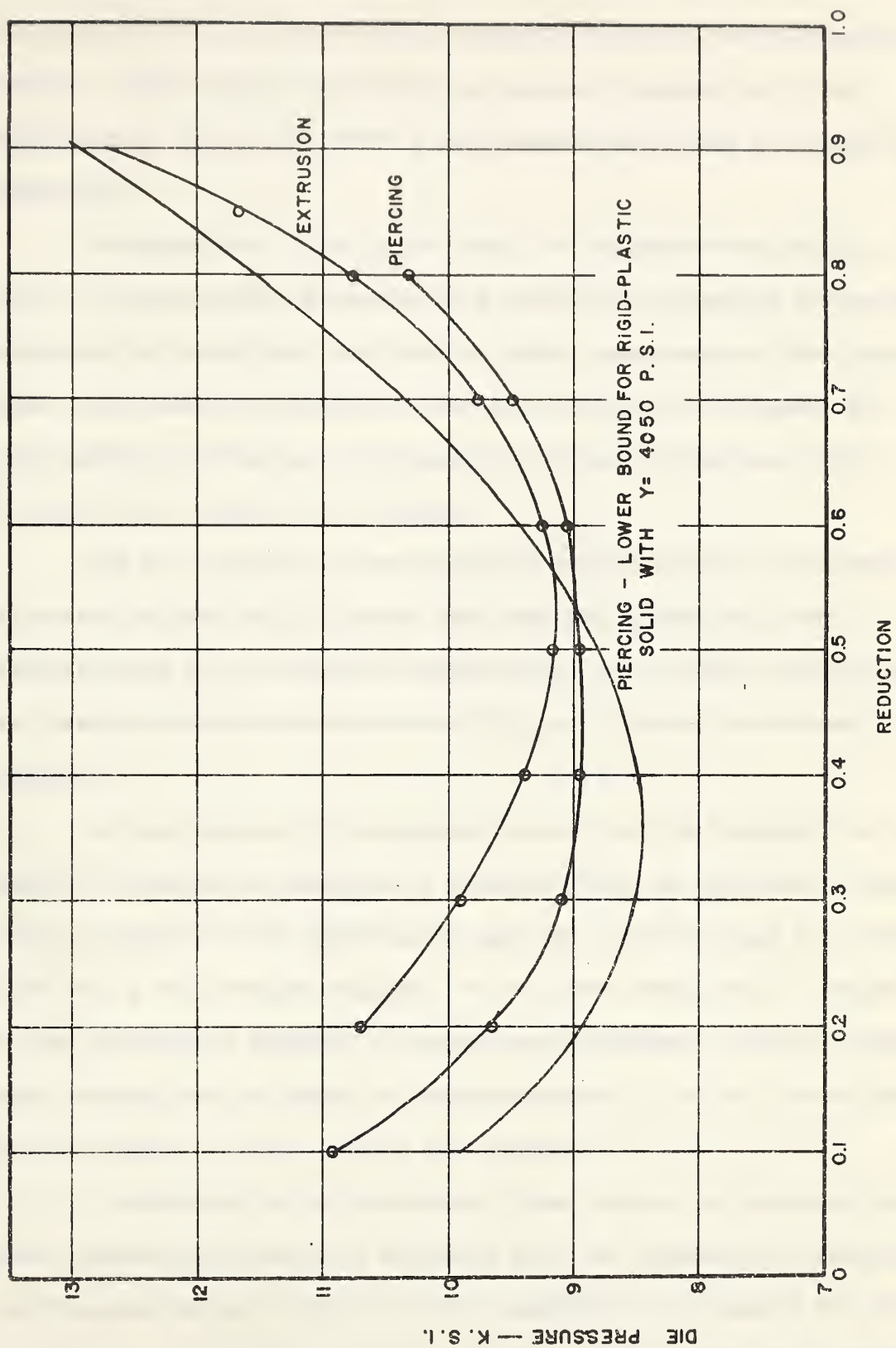


FIGURE 16. PRESSURE-REDUCTION DIAGRAM FOR ANNEALED TELLURIUM LEAD

The P-r diagrams for the piercing of annealed and fully-hardened tellurium lead do not possess the similarity found for the extrusion results. Other than the fact that the piercing diagrams are both approximately symmetrical about a reduction of 0.45, they are completely dissimilar.

A comparison of the lower bound, due to Haddow and Johnson, with the experimentally determined P-r relation for piercing cold-worked tellurium lead shows that the bound is rather conservative. The lower bound does, however, substantiate the fact that the P-r diagrams for axi-symmetric piercing are not symmetrical about a reduction of 0.5, as plane strain theory would indicate.

The P-r diagrams for the extrusion and piercing of cold-worked tellurium lead are similar except that they are symmetrical about different axes and are displaced vertically. For a given reduction the die pressures of extrusion are about 750 p.s.i. greater than those for piercing.

No such similarity is apparent between the P-r diagrams for the inverted extrusion and piercing of annealed lead. As previously stated, the P-r diagram for the extrusion of annealed tellurium lead is a smooth curve with a well defined minimum. On the other hand, the P-r diagram for the piercing of annealed tellurium lead possesses a very flat minimum which extends over the range of reductions from 0.3 to 0.6. There seems to be no reason to expect such a flat minimum.

A comparison of the theoretical plane strain die pressures with those obtained experimentally indicates that the theoretical plane strain die pressures are not close to the axi-symmetric die pressures for the same reduction. For example, the theoretical plane strain die pressure for a 0.5 reduction by either piercing or extrusion is $(2 + \pi)K$. The

working material is assumed to be a rigid-plastic, non-hardening solid. Applied to the fully-hardened material used in these experiments, and using Mises yield criteria, this produces a die pressure of 12,000 p.s.i. The value of 12,000 p.s.i. is considerably in error with the experimental die pressures 13,250 p.s.i. and 13,850 p.s.i. for piercing and extrusion.

8.5. Mean Equivalent Strains

Mean equivalent strains, $(\frac{P_r}{Y} = [\bar{e}^P])$, were calculated for both the piercing and inverted extrusion of cold-worked tellurium lead. P values were obtained from Fig. 15. The initial roundness of the stress-strain diagram (Fig. 14) for the cold-worked material was neglected and Y was taken as 4050 p.s.i. for all reductions.

Figure 17 shows the mean equivalent strains which were calculated. The mean equivalent strains for a given reduction are, of course, in the same ratios as are the corresponding die pressures.

Following the method of (3.2) and using the above values of mean equivalent strain an empirical work per unit volume was calculated for the extrusion and piercing of annealed tellurium lead. This empirical work is termed the mean equivalent work to distinguish it from the experimentally determined value of plastic work per unit volume.

These two values of plastic work are compared in Fig. 18. In all cases the mean equivalent value exceeds the actual value; the error ranging from five percent for the low reductions to fifteen percent for the higher reductions.

The fact, that in these experiments the mean equivalent work provides an acceptable upper bound to the actual work, should not be considered as a general property of mean equivalent work. Haddow and Johnson¹⁶ have, for instance, presented results for the axi-symmetric

The first of these is the fact that the
 system is not a simple one, and that
 the results are not always the same.
 The second is that the system is not
 always the same, and that the results
 are not always the same.

The third is that the system is not
 always the same, and that the results
 are not always the same.

The fourth is that the system is not
 always the same, and that the results
 are not always the same. The fifth is
 that the system is not always the same,
 and that the results are not always the
 same. The sixth is that the system is
 not always the same, and that the
 results are not always the same.

The seventh is that the system is not
 always the same, and that the results
 are not always the same. The eighth is
 that the system is not always the same,
 and that the results are not always the
 same.

The ninth is that the system is not
 always the same, and that the results
 are not always the same. The tenth is
 that the system is not always the same,
 and that the results are not always the
 same. The eleventh is that the system
 is not always the same, and that the
 results are not always the same.

The twelfth is that the system is not
 always the same, and that the results
 are not always the same. The thirteenth
 is that the system is not always the same,
 and that the results are not always the
 same.

The fourteenth is that the system is not
 always the same, and that the results
 are not always the same. The fifteenth
 is that the system is not always the same,
 and that the results are not always the
 same.

The sixteenth is that the system is not
 always the same, and that the results
 are not always the same. The seventeenth
 is that the system is not always the same,
 and that the results are not always the
 same.

The eighteenth is that the system is not
 always the same, and that the results
 are not always the same. The nineteenth
 is that the system is not always the same,
 and that the results are not always the
 same. The twentieth is that the system
 is not always the same, and that the
 results are not always the same.

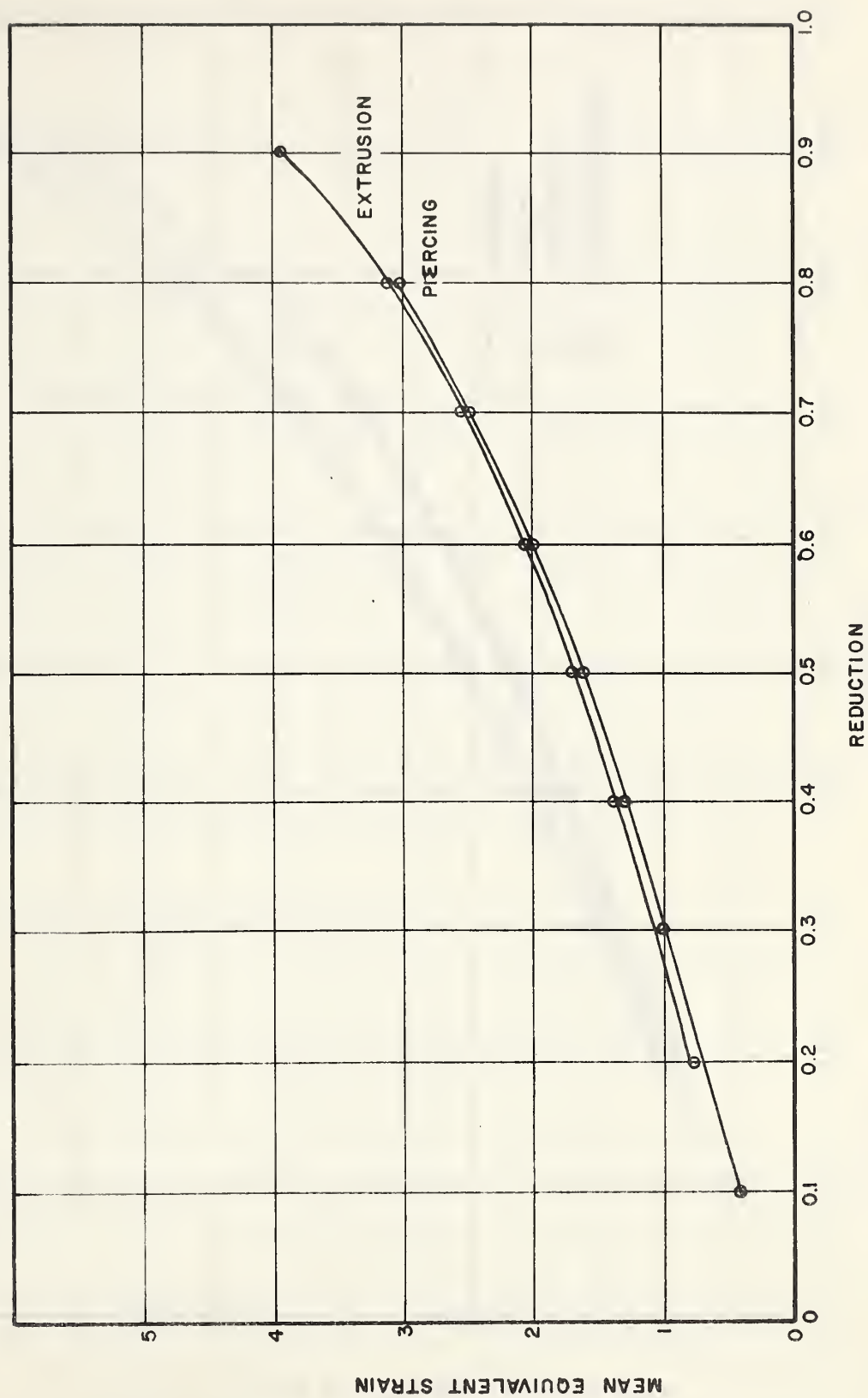


FIGURE 17. MEAN EQUIVALENT STRAINS FOR FULLY-HARDENED TELLURIUM LEAD

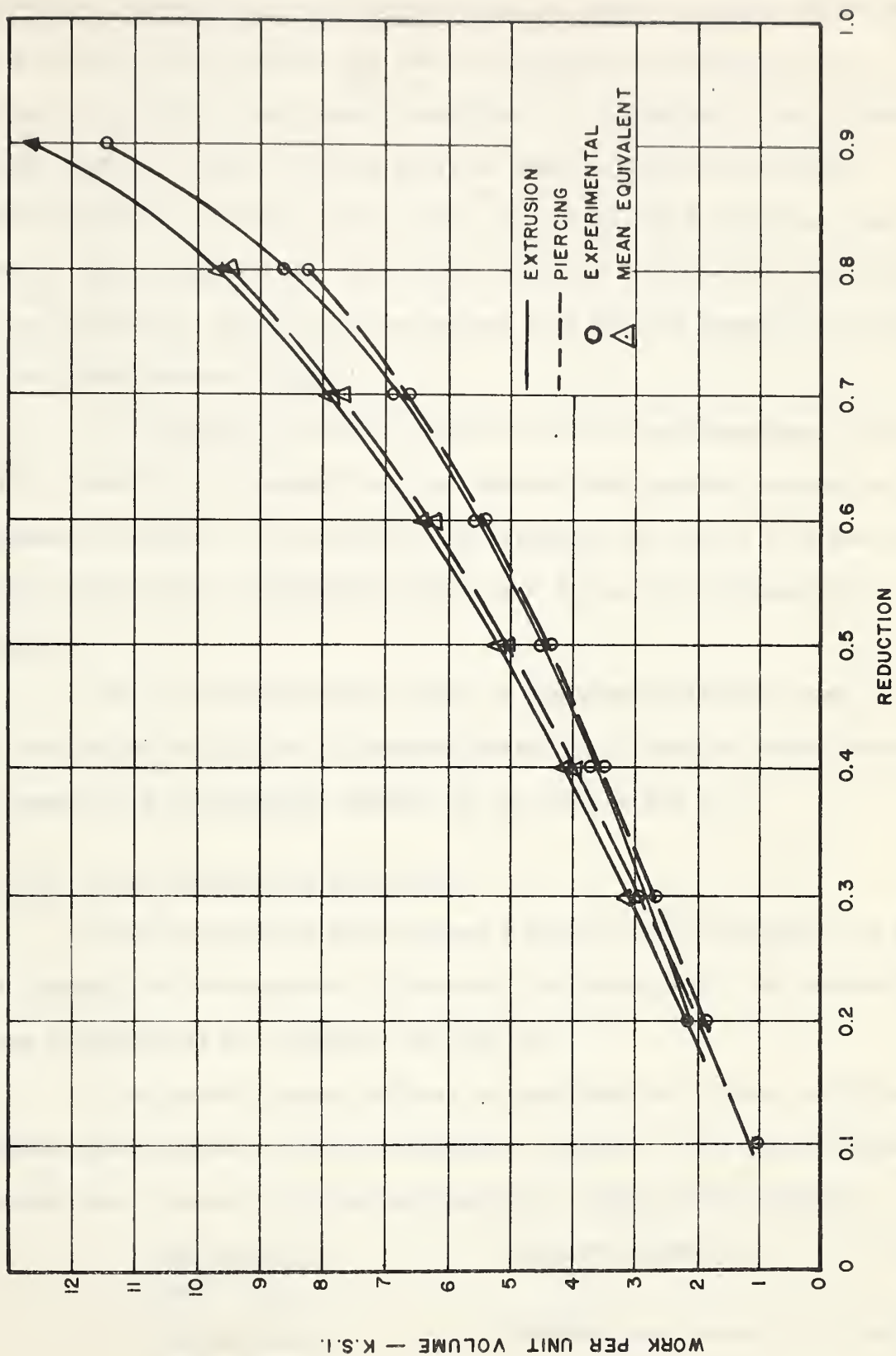


FIGURE 18. COMPARISON OF EXPERIMENTAL AND MEAN EQUIVALENT PLASTIC WORK—ANNEALED TELLURIUM LEAD

piercing of annealed 0.065 tellurium lead, in which, the mean equivalent work varied from 15 percent too low for the smaller reductions to 20 percent too high for the larger reductions. A comparison of the stress-strain diagrams showed that the material used by Haddow and Johnson work-hardened to a greater extent than did the annealed tellurium lead used in these experiments. This would therefore indicate that the success to be achieved in using a mean equivalent work largely depends on the shape of the stress-strain diagram.

P-r diagrams are often presented in the non-dimensional form of $P/\bar{Y} - r$, where it is assumed that the plastic work per unit volume may be obtained from $\bar{Y}[\bar{e}^P]$, (Eq. 3.10a). As explained in (3.2.), \bar{Y} is the average yield stress over a logarithmic strain of $[\bar{e}^P]$ on the stress-strain diagram.

Due to the significant error in the mean equivalent work, $\bar{Y}[\bar{e}^P]$, for the larger reductions of **annealed material**, it was not deemed reasonable to present the experimental results in the form of $P/\bar{Y} - r$.

8.6. Ideal Deformation Efficiency

Ideal deformation efficiencies (Eq.2.6) were calculated for both the piercing and extrusion of cold-worked tellurium lead. The results of these calculations are presented in Fig. 19.

The plotted points indicate an approximately linear variation between the efficiency and the reduction. Using the best straight line through these points the following empirical formulas were obtained.

$P = \frac{49Y \ln 1/1-r}{18r^2 + 11r}$	Inverted Extrusion.....8.1
$P = \frac{50Y \ln 1/1-r}{18r^2 + 12r}$	Piercing8.2

These relationships provide good accuracy over the range of reductions from 0.1 to 0.9 using cold-worked material.

Unfortunately, as stated in (8.5), the mean equivalent strains derived from these formulas could not be used to calculate acceptable mean equivalent work values for the annealed material.

In order to test the reproducibility of experimental results, the mean equivalent strains as calculated from Eq. 8.1 were compared with those obtained from Eq. 2.3 due to Dodeja and Johnson. For reductions of 0.5 and 0.9 the values of mean equivalent strain differed by eight and two percent respectively.

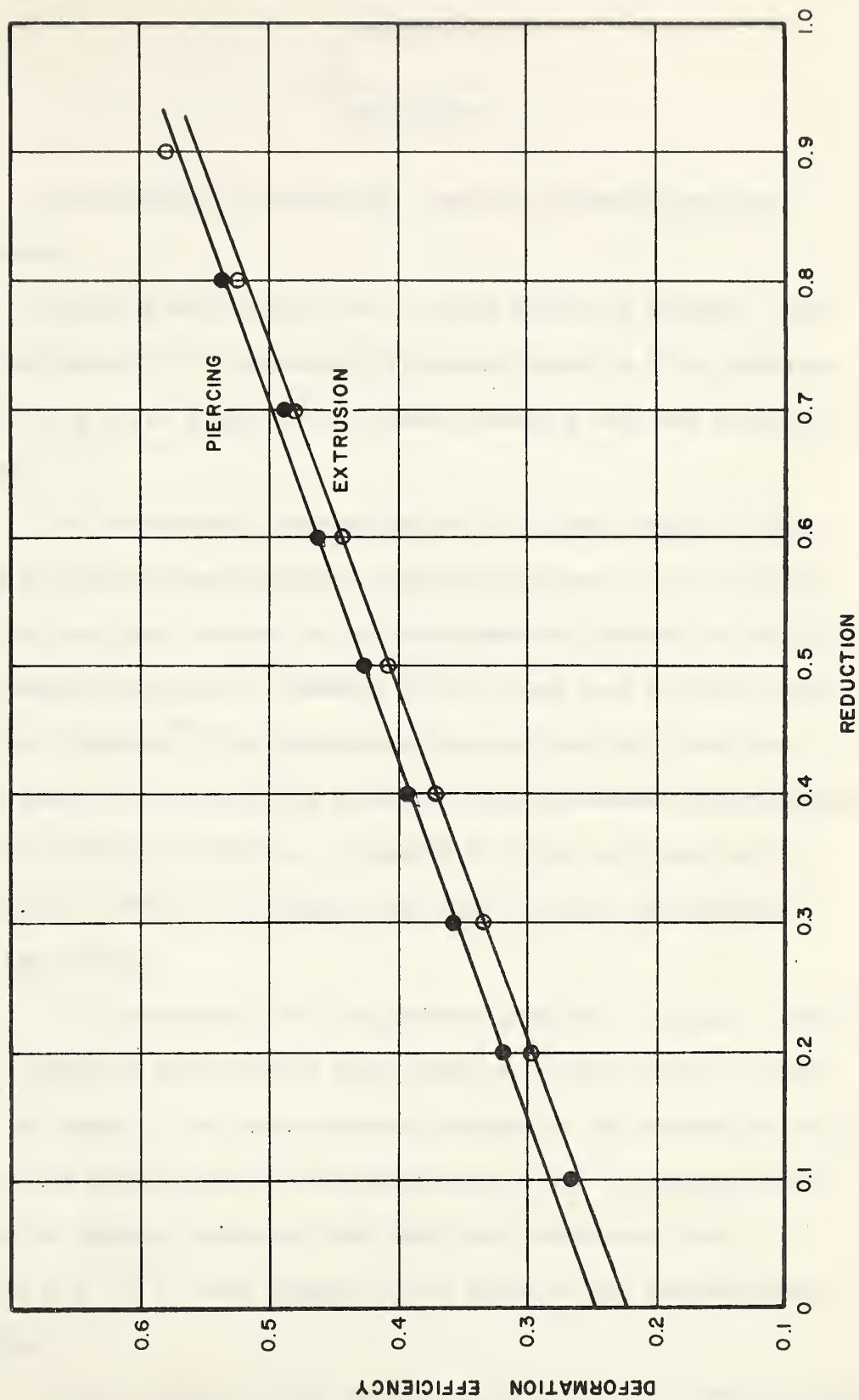


FIGURE 19. DEFORMATION EFFICIENCIES FOR FULLY-HARDENED TELLURIUM LEAD



CHAPTER 9

CONCLUSIONS

Axi-symmetric piercing and inverted extrusion have been compared.

Piercing was found to be the most efficient process. For both processes the deformation efficiency, based on a die pressure of $\frac{Y}{r} \ln \frac{1}{1-r}$, was found to vary almost linearly with the reduction of area.

The experimental results showed that plane strain theory, assuming frictionless die faces and container walls, could not be applied with good results to the axi-symmetric problems of piercing and inverted extrusion. However, it was found that a plane strain solution (Johnson²⁷) for reductions greater than 0.67 predicted die pressures to within five percent of those obtained experimentally for axi-symmetric extrusion. Johnson's solution was based on the assumptions that the die faces were rough and that the container bore was smooth.

It is concluded that the success obtained in using a common mean equivalent strain for a given working process largely depends upon the shape of the stress-strain diagram for the working material (hence the work-hardening characteristics of the working material). Hence the accuracy achieved from empirical formulas of the form $P_r = \bar{Y} [\bar{e}^{-P}]$ also depends on the shape of the stress-strain diagram.

It was found that the friction drag associated with piercing is not always negligible, even with proper lubrication.

Dead Metal was observed in the ~~a~~xi-symmetric inverted
extrusion experiments for reductions below 0.5.

BIBLIOGRAPHY

1. R.Hill, "Mathematical Theory of Plasticity", Oxford (Claredon Press) 1960, p. 134.
2. Ibid., p. 263.
3. P.S.Symonds, "On the General Equations of Axial Symmetry in the Theory of Plasticity", Quarterly Journal of Applied Mathematics, vol. 6, 1949, pp. 448-452.
4. N.W.Purchase and S.J.Tupper, "Experiments with a Laboratory Apparatus Under Conditions of Plane Strain", Journal of the Mechanics and Physics of Solids, vol. 1, 1953, p. 280.
5. C.E.Pearson, "The Extrusion of Metals", John Wiley and Sons, Inc., New York, N.Y., 1944, p. 120.
6. L.C.Dodeja and W. Johnson, "The Cold Extrusion of Circular Rods Through Square Multiple Hole Dies", Journal of the Mechanics and Physics of Solids, vol. 5, 1957, p. 294.
7. Ibid., p. 288.
8. Ibid.
9. R.Hill, "The Theory of the Extrusion of Metals", Selected Government Research Reports, vol. 6, Strength and Testing of Materials, pt.1, p. 200.
10. C.E.Pearson and R.N.Parkins, "The Extrusion of Metals", John Wiley and Sons, Inc., New York, N.Y., 1960, p. 215.
11. R. Hill, "Mathematical Theory of Plasticity", Oxford (Claredon Press), 1960, pp. 30-33.
12. E.G.Thomsen, "Plasticity Equations and Their Application to Working of Metals in the Work-Hardening Range", Trans. A.S.M.E., vol. 78, 1956, p. 411.
13. E.G.Thomsen and J. Frisch, "Stresses and Strains in Cold-Extruding 2S-O Aluminum", Trans. A.S.M.E., vol. 77, 1955, p. 1344.
14. W. Johnson, "Experiments in Plane Strain Extrusion", Journal of the Mechanics and Physics of Solids, vol. 4, 1956, p. 281.
15. Dodeja and Johnson, op. cit., p. 289.
16. J.B.Haddow and W. Johnson, "Experiments in the Piercing of Soft Metals", Proceedings of the Second International Machine Tool Design and Research Conference, Manchester, 25-29 September, 1961.

17. R. Hill, "Mathematical Theory of Plasticity", Oxford (Clarendon Press), 1960, pp. 60-69.
18. Haddow and Johnson, op. cit.
19. J.B.Haddow and W. Johnson, "On the Axi-Symmetric Piercing Process", International Journal of Mechanical Sciences, In Press.
20. J.B.Haddow and W. Johnston, "Experiments in the Piercing of Soft Metals", Proceedings of the Second International Machine Tool Design and Research Conference, Manchester, 25-29 September, 1961.
21. Ibid.
22. W. Hofmann and H. Hanemann, Summary of Metallurgical Review, vol. 6, No. 23, 1961, p. 341.
23. Hill, op. cit., p. 27.
24. Ibid., p. 277.
25. Haddow and Johnson, op. cit.
26. N. Loizou and R.B.Sims, "The Yield Stress of Pure Lead in Compression", Journal of the Mechanics and Physics of Solids, vol. 1, 1953, pp. 234-243.
27. W. Johnson, "Extrusion through square Dies of Large Reduction", Journal of the Mechanics and Physics of Solids, vol. 4, 1956, p. 198.

B29797